Davies, P. J., McKenzie, J. A., Palmer-Julson, A., et al., 1991
Proceedings of the Ocean Drilling Program, Initial Reports, Vol. 133

17. SITE 824[1]

Shipboard Scientific Party[2]

HOLE 824A

Date occupied: 1 October 1990

Date departed: 3 October 1990

Time on hole: 2 days, 5 hr, 24 min

Position: 16°26.704'S, 147°45.737'E

Bottom felt (rig floor; m, drill-pipe measurement): 1011.9

Distance between rig floor and sea level (m): 11.47

Water depth (drill-pipe measurement from sea level, m): 1000.4

Total depth (rig floor; m): 1389.2

Penetration (m): 377.3

Number of cores (including cores with no recovery): 36

Total length of cored section (m): 327.3

Total core recovered (m): 129.7

Core recovery (%): 39.6

Oldest sediment recovered:
Depth (mbsf): 377.3
Nature: bioclastic rudstone
Age: Miocene to late Oligocene

HOLE 824B

Date occupied: 3 October 1990

Date departed: 3 October 1990

Time on hole: 7 hr, 20 min

Position: 16°26.703'S, 147°45.720'E

Bottom felt (rig floor; m, drill-pipe measurement): 1013.5

Distance between rig floor and sea level (m): 11.57

Water depth (drill-pipe measurement from sea level, m): 1001.9

Total depth (rig floor; m): 1066.0

Penetration (m): 52.5

Number of cores (including cores with no recovery): 6

Total length of cored section (m): 52.5

Total core recovered (m): 53.5

Core recovery (%): 101.5

Oldest sediment recovered:
Depth (mbsf): 9.41
Nature: bioclastic packstone
Age: Pleistocene

HOLE 824C

Date occupied: 3 October 1990

Date departed: 3 October 1990

Time on hole: 1 day, 8 hr, 3 min

Position: 16°26.705'S, 147°45.753'E

Bottom felt (rig floor; m, drill-pipe measurement): 1011.9

Distance between rig floor and sea level (m): 11.57

Water depth (drill-pipe measurement from sea level, m): 1000.3

Total depth (rig floor; m): 1444.3

Penetration (m): 430.8

Number of cores (including cores with no recovery): 19

Total length of cored section (m): 183.2

Total core recovered (m): 3.2

Core recovery (%): 1.1

Oldest sediment recovered:
Depth (mbsf): 401.9
Nature: muddy quartz bioclastic sandstone
Age: Miocene to late Oligocene

Hard rock recovered:
Depth (mbsf): below 401.9
Nature: phyllite

HOLE 824D

Date occupied: 4 October 1990

Date departed: 6 October 1990

Time on hole: 1 day, 6 hr, 52 min

Position: 16°26.690'S, 147°45.753'E

Bottom felt (rig floor; m, drill-pipe measurement): 1013.5

Distance between rig floor and sea level (m): 11.57

Water depth (drill-pipe measurement from sea level, m): 1001.9

Total depth (rig floor; m): 1444.5

Penetration (m): 431.0

Number of cores (including cores with no recovery): 10

Total length of cored section (m): 96.5

Total core recovered (m): 1.1

Core recovery (%): 1.1

Hard rock recovered:
Depth (mbsf): below 401.9
Nature: phyllite
Age: unknown

Principal results: Site 824 is located in 1004 m of water on the western slope of the Queensland Plateau west of Holmes Reef. It represents a slope site intended to provide an understanding of processes along the eastern margin of the Queensland Trough and a nearly complete section of Paleogene sediments and the basement onto which they have transgressed. Four holes were drilled to a total depth of 431 meters below seafloor (mbsf): Hole 824A was drilled with APC/XCB after washing down to 50 mbsf; Hole 824B used APC coring to recover the top 50 mbsf, and Holes 824C and 824D used RCB coring to recover the sections below 300 mbsf, including the basement.

The odd sequence of drilling defined above was due to the shortage of core liners aboard the vessel. The sediments range in

[1] Davies, P. J., McKenzie, J. A., Palmer-Julson, A., et al., 1991. *Proc. ODP, Init. Repts.*, 133: College Station, TX (Ocean Drilling Program).
[2] Shipboard Scientific Party is as given in list of participants preceding the contents.

age from late Pleistocene to the late Oligocene–early Miocene. Basement of probable Paleozoic age(?) was reached. Benthic foraminifers indicate that the sediments were deposited entirely within middle bathyal depths. Recovery averaged 28.4% for Site 824. Sedimentation rates were highest during the late Pleistocene if one assumes that the seafloor has a Holocene age. Thereafter, rates decrease to 12.9 cm/k.y. by 2.4 Ma before an increase to 22–30 cm/k.y. for the section down to 11 Ma.

Sediments recovered at Site 824 are pure carbonates deposited as nannofossil oozes and allochthonous packstones and rudstones composed of mollusks, bryozoans, corals, and coralline algae. Seven lithologic units have been recognized on the basis of the dominance of the two depositional styles and facies:

1. *Unit I:* depth, 0–105 mbsf; age, Pleistocene. Unit I is characterized by discrete layers and intervals of redeposited bioclastic packstone and rudstone separated by intervening periplatform oozes and chalks, that consist of a mixture of 40% to 60% fine bank-derived aragonite particles and variable proportions of planktonic particles, nannofossils, foraminifers, and in the upper few meters of Site 824, pteropod tests. Unit I consists of two major 45- to 50-m-thick, upward-fining packages. The lower part of each package consists of a thick homogeneous interval of bioclastic redeposited packstone sediments (Subunits IB and ID), whereas the upper part of each package consists of alternating thin layers of bioclastic redeposited sediments and discrete intervals of periplatform oozes and chalks (Subunits IA and IC).

Subunit IA: depth, 0–27 mbsf; age, Pleistocene. Subunit IA is characterized by intervals of white periplatform oozes and chalks, ranging in thickness from 20 to 60 cm and intercalated between numerous bioclastic layers.

Subunit IB: depth, 27–52 mbsf; age, Pleistocene. Subunit IB consists mostly of bioclastic packstone redeposited sediments with foraminifers, nannofossils, and micrite. Grain size variations show a coarsening upward trend from very fine sand-sized bioclastic grains to very coarse sand-sized grains and, finally, to silt and gravel sized grains.

Subunit IC: depth, 52–68 mbsf; age, Pleistocene. The lithologies in Subunit IC resemble the ones described in Subunit IA. Subunit IC consists of numerous 5–145-cm-thick (average 60-cm) layers of bioclastic redeposited packstone sediments separated from one another by 20- to 40-cm-thick intervals of periplatform oozes and chalks.

Subunit ID: depth, 68–105 mbsf; age, Pleistocene. Subunit ID consists of homogeneous, white, unlithified bioclastic redeposited packstone sediments with abundant fragments of *Halimeda* and bryozoans.

2. Unit II: Depth, 105–135.5 mbsf; age, late Pliocene. Unit II consists of numerous discrete layers of redeposited bioclastic packstone separated by intervening periplatform oozes and chalks, that consist of a mixture of up to 40% fine bank-derived aragonite particles (micrite) identified by X-ray diffraction and variable proportions of planktonic particles, nannofossils, and foraminifers. Bioclastic grains in the redeposited layers consist of shallow-water carbonate fragments of corals, bryozoans, echinoderms, and mollusks. Frequency of redeposited layers varies within Unit II.

3. *Unit III:* depth, 135.5–166 mbsf; age, Pliocene. Unit III is defined in a poorly recovered interval of Hole 824A. Unit III consists of white, very pale brown to dark gray, well-cemented, limestone pieces, possibly created by drilling, that contain clasts of bioclastic rudstone and packstone. Allochems consist of large fragments of corals (centimeter size), encrusting and branching corallinacean algae, as well as complete rhodoliths 3 cm in diameter, embedded in a sand-size bioclastic packstone matrix.

4. *Unit IV:* depth, 166–242.3 mbsf; age, middle to late Miocene. Unit IV consists of very white to light gray nannofossil oozes and chalks with variable proportions of bioclasts and micrite. Aragonite in trace amount is present only in the upper part of Unit IV. Layers of fine to medium sand sized, redeposited carbonate particles are very pale brown in color. Graded bedding is often not observed, although the bases of redeposited layers are usually more distinct and their tops more gradational. Shallow-water components are abundant, i.e., corals, large foraminifers, coralline algae, alcyonarian spicules, mollusks, and echinoids. Subunit IVA (Cores 133-824A-14H and -15H) is distinguished from Subunit IVB (Cores 133-824A-15H and -21X) by the occurrence of redeposited packstone layers in Subunit IVA, whereas redeposited layers do not clearly occur in Subunit IVB.

5. *Unit V:* depth, 242.3–338.7 mbsf, age, middle to late Miocene. Unit V can be subdivided into two subunits on the basis of the occurrence of planktonic foraminifers and several distinct layers of redeposited sediments in Subunit VA, whereas planktonic foraminifers and layers of clearly redeposited sediments are not observed in Subunit VB.

Subunit VA: depth, 242.3–309.9 mbsf; age, middle to late Miocene. Subunit VA consists of alternating very white, foraminifer (planktonic) chalk and white to very pale brown beds of redeposited, shallow-water-derived, carbonate grains (mollusks, corals, corallinacean algae, fragments or complete rhodoliths [3 cm in diameter] with laminar coating, fragments of (?)*Halimeda* as molds, larger foraminifers [Alveolinidae], small miliolids, and textulariids). Well-rounded, isolated, litholclasts of up to 3 cm in diameter also were observed embedded in planktonic foraminifer chalks.

Subunit VB: depth, 309.9–338.7 mbsf; age, middle to late Miocene. Subunit VB consists of white to very pale brown, dense skeletal packstone and rudstone. Most common grains are branching corals, pelecypods, gastropods, echinoids, benthic foraminifers (miliolids and larger foraminifers, i.e., Alveolinidae), encrusting and branching corallinacean algae, and complete rhodoliths. Floatstones with branching corals thinly encrusted by corallinacean algae occur at the base of Subunit VB. Coral and mollusk fragments are preserved as molds throughout Subunit VB. Quartz grains occur at some levels.

6. *Unit VI:* depth, 338.7–401.9 mbsf; age, Miocene to late Oligocene. Unit VI consists of very white bioclastic branching bryozoan-rich rudstone with poorly preserved corallinacean algal, mollusk, larger foraminifer, and tiny branching (ahermatipic?) coral fragments. Grain size ranges from sand to granules. In addition, angular quartz grains occur throughout Unit V. The color of the very poorly sorted quartz bioclastic sandstone with muddy matrix at the base of Unit VI ranges from a dark yellowish brown to gray. Identifiable carbonate grains are fragments of bryozoans and larger foraminifers. Lithoclasts of reworked black phyllite, several mm in diameter, occur within the base of Unit V.

7. *Unit VII:* depth, 401.9–431 mbsf; age, unknown. The upper part of Unit VII consists of a deeply weathered, mottled orange and brown regolith, a fine-grained rock with 1-mm-sized quartz grains. The regolith covers black to very dark gray carbonaceous and quartzose, as well as chloritic, phyllites characterized by intense crenulation, kink bands, microfaults, and irregular transverse quartz and calcite veins. Light gray, finely crystalline metavolcanic rock of possible basic composition is intercalated within the phyllites with common pyrite occurrence at the lithologic contacts.

Interstitial water chemistry of the cores shows that calcium and magnesium change little, either as a result of seawater contamination or because of fluid flow in the hole. Concentrations of strontium increased three times by 21.95 mbsf and then gradually decreased toward the bottom of the hole. Potassium shows no change, reflecting the lack of clay minerals in the cores. Values of alkalinity, sulfate, and ammonia also exhibit little change.

X-ray diffraction analyses indicate that from 0 to 119.4 mbsf, sediments contain more than 40% aragonite; however, below 257.2 mbsf, aragonite is absent. Calcite increases from 24.22% near the top of the hole to 100% at its base. Small amounts of dolomite occur between 95.4 and 238.6 mbsf, whereas calcium carbonate varies cyclically with depth.

The percentage of organic carbon in the sediments is low (<0.25%). These sediments also contain low concentrations of methane (2–12 ppm), while ethane and propane were not detected.

BACKGROUND AND SCIENTIFIC OBJECTIVES

Drilling on the Queensland Plateau was last conducted during Leg 21 of the Deep Sea Drilling project (Burns, Andrews, et al., 1973). Drilling at DSDP Site 209 defined three lithologic facies (see Fig. 2, "Site 811" chapter, this volume). A basal upper bathyal to neritic upper middle Eocene glauconite-bearing bioclastic and foraminifer-rich sediment is overlain by an uppermost middle to upper Eocene section comprised of terrigenous detritus and foraminifer ooze, suggesting subsidence in the upper upper Eocene to upper Oligocene. The hiatus was followed by further subsidence to the present mid-bathyal depths and deposition of almost pure foraminifer and nannofossil ooze from the late Oligocene to the present, with a period of apparent nondeposition or erosion in the middle Miocene. The most important conclusions to emerge from the drilling at DSDP Site 209 were:

1. The site clearly records the subsidence history of the Queensland Plateau from shallow neritic depths in the late middle Eocene to its present mid-bathyal depth of 1428 m (see Fig. 2, "Site 811" chapter, this volume); a major subsidence pulse began in the latest part of the middle Miocene.
2. The sediments are dominantly foraminifer ooze throughout with the terrigenous content of the cores decreasing in the upper units, but particularly from the middle to upper Eocene.
3. A major period of nondeposition or submarine erosion spans most of the Oligocene, after which deposition is almost entirely carbonate dominated.
4. The Oligocene unconformity is thought to be related to circulation changes in the southwest Pacific.

Studies at DSDP Site 209 raised many questions. In particular, they showed an apparent lack of correlation between unconformities and seismic reflectors. They also failed to answer questions regarding the nature of the basement beneath the Queensland Plateau. Both questions are still very pertinent today.

Site 824 lies in 1000.3 m of water on the western margin of the Queensland Plateau west of Holmes Reef. Site survey seismic data throughout the site are shown in Figure 1. Site 824 presents an opportunity to define a record of plateau sedimentation through the late Neogene and the extent to which sea level affected sedimentation during the late Oligocene and early Miocene (see Fig. 2). Other objectives were to define the beginning of shallow-water carbonate sedimentation on the plateau and, in particular, the time at which tropical reefs started to develop; to determine whether the carbonate system at Holmes Reef began as a tropical or a temperate buildup; and to define the origin of the Queensland Plateau by drilling into basement, which is thought to be composed of Paleozoic rocks (Mutter and Karner, 1980). Beneath the western third of the plateau, and particularly near Site 824, basement is progressively downfaulted toward the Queensland Trough (see Fig. 3, "Site 811" chapter, this volume). Basement rocks were almost certainly exposed and planated during Cretaceous and Paleocene time.

The principal objectives of drilling at Site 824 were:

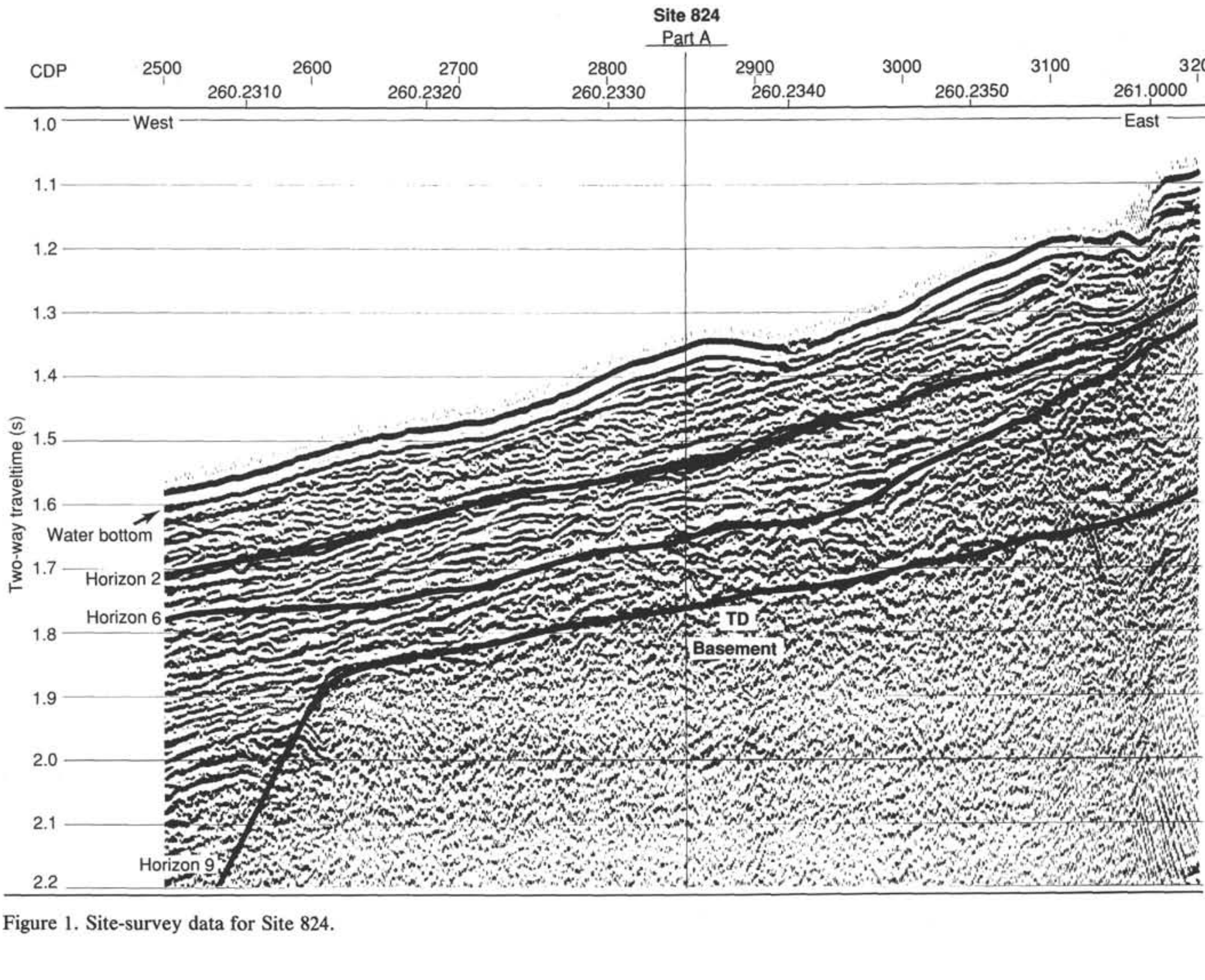

Figure 1. Site-survey data for Site 824.

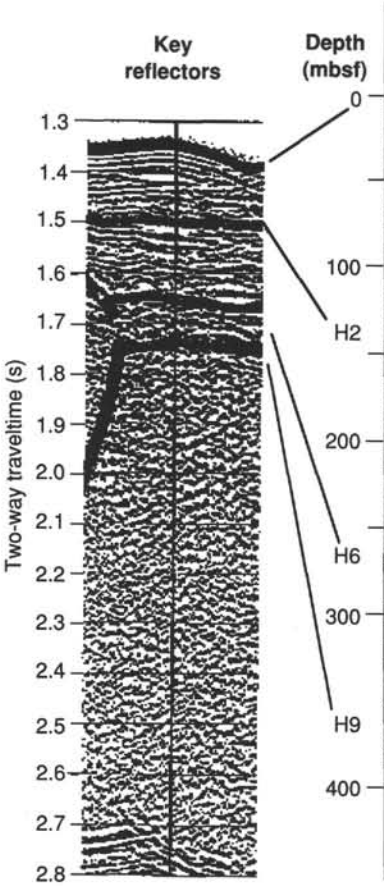

	Age	Velocity (km/s)	Lithology	Paleoenvironment	Sed. rate (m/m.y.)	Comments
	Quaternary	1.55	Current-winnowed carbonate sand and mud	Pelagic plateau slope	21.0	(?) Contourite
	(62) latest Miocene and Pliocene	1.75	Interbedded carbonate sand and mud possibly with some gravel	Pelagic toe of slope	17.5	Periplatform deposits
	(149) (?) late Miocene	1.80	As above, but with more gravel	Pelagic	9.0	Periplatform deposits
	(203) late early middle Miocene	2.10	Carbonate gravel, sand	Hemipelagic midslope	10.5	Periplatform deposits
	(266) latest Oligocene to early Miocene	2.20	Rudstone, wackestone, and packstone	Carbonate platform slope	12.5	Debris apron
	(365) (?) Paleozoic		Low-grade metasediment			Basement
TD	(390)					

Figure 2. Pre-drilling prognosis for Site 824.

1. To determine the age and facies of upper slope deposits adjacent to a plateau margin reefal build-up.
2. To determine the paleoceanographic and paleoclimatic signal within a periplatform system.
3. To understand slope processes in an exclusively carbonate depositional system.
4. To determine the composition and age of basement.

Previously available data in the region includes that collected by BMR since 1971 together with a few long regional Shell and GSI seismic lines. Better quality seismic data were collected in 1987 for the ODP site survey (BMR Line 75/037); cores collected during that same cruise (75GC/22 and 75GC/23) define the surface sediments as foraminiferal oozes. There were no reasons to expect hydrocarbon accumulations at the site because of the shallow basement, the absence of structural closure, and a relatively thin thermally immature sedimentary section. Thus no major safety risks were anticipated in drilling Site 824, although some minor biogenic gas was expected.

OPERATIONS

Transit to Site 824

The sea voyage to Site 824 (proposed site NEA-6) began at 2342L (all times reported in this section are in local time, or L) 30 September, and covered 50 nmi in 5.2 hr at 9.6 kt average speed. A seismic survey was run over Site 824 covering 10 nmi in 2.1 hr at an average speed of 4.8 kt. A Datasonics beacon was dropped at 0806L, 1 October 1990.

Hole 824A

Hole 824A was located at 16°26.704′S, 147°45.737′E; from precision depth recorder (PDR) analyses we predicted a water depth of 997.9 m below sea level (mbsl). A used 11-7/16-in. Security four-cone insert bit was run with the standard APC/XCB bottom-hole assembly (BHA), nonmagnetic drill collar, four 8-1/4-in. drill collars, and Hydrolex jars with two drill collars above. The bit was lowered to a water depth of 995.5 mbsl for the first shot. Hole 824A was spudded at 1123L 1 October. The first core recovered 4.6 m of sediment, indicating that the mud line occurs at 1000.4 mbsl. As core liners were in short supply, the decision was made to attempt to reach the deeper objectives at this site first; then, as the liner supply allowed, the shallow part of the section would be cored. Therefore, the first core liner was washed clean of sediment for later reuse. The hole was drilled from 0.0 to 35.0 mbsf. A partial core was taken from 35.0 to 40.0 mbsf but recovered no sediment. The hole was drilled to 50.0 mbsf, and continuous APC cores (133-824A-1H through -10H) were taken from 50.0 to 137.9 mbsf, with 87.9 m cored and 85.9 m recovered (97.7% recovery). APC coring ended when a hard layer was reached, resulting in a partial stroke and a split liner. Cores 133-824A-11X through -13X were taken from 137.9 to 165.7 mbsf, with 27.8 m cored and 0.1 m recovered (0.4% recovery). Below this level sediment was soft, and the decision was made to return to APC coring. Cores 133-824A-14H and -15H were taken from 165.7 to 184.7 mbsf, with 19.0 m cored and 18.4 m recovered (96.7% recovery). Core 133-

824A-15H was a partial stroke, indicating an encounter with additional hard material.

Cores 133-824A-16X through -36X were taken from 194.0 to 377.3 mbsf, with 192.6 m cored and 24.3 m recovered (12.6% recovery). The pipe became stuck with the bit on the bottom after coring Core 133-824A-36X; the core had been cut with a low circulation rate in an attempt to improve extremely poor recovery in the unconsolidated, coarse-grained carbonates.

A 40-bbl gel sweep was circulated at 400 gpm and 2300 psi, and the pipe was worked to 170,000 lb overpull (450,000 indicator weight). The Hydrolex jars were engaged, and jarring was alternated with circulating mud sweeps while working the pipe. The jars hit 38 blows up with 100,000–150,000 lb, and 18 blows down with 40,000 lb. A total of 200 bbl of mud were circulated at as much as 400–600 gpm and 2300–2895 psi, with 170,000–460,000 lb overpull (740,000 lb indicator weight). The maximum allowable indicator overpull was 774,000 lb. The drill string moved 10 m in 4 hr, but showed no further response. We think that the low circulation rate initially contributed to packing off the annulus, permitting cobbles of hard sediment to settle and stick around the BHA. This was the fourth severe stuck pipe incident this leg, all having occurred in unconsolidated coarse-grained carbonates. Although the jars were still working and marginal progress had been made in working the pipe off the bottom, a decision was made to back off the drill string to conserve time.

A "stringshot" explosive charge was run to the bottom of the nonmagnetic drill collar, but failed to back off the drill string. A second charge was run to the drill collar below the jars, and succeeded in backing off the drill collar so the remainder of the drill string could be recovered.

Hole 824B

The ship was moved 25 m west, and an APC/XCB BHA was run in the hole. Hole 824B was located at 16°26.703′S, 146°45.720′E. The bit was lowered to a water depth of 997.4 mbsl for the first shot. Hole 824B was spudded at 1815L 3 October. Core 133-824B-1H recovered 4.6 m of sediment, indicating that the mud line occurs at a water depth of 1001.9 mbsl. Continuous APC cores (Cores 133-824B-1H through -6H) were taken from 0.0 to 52.5 mbsf, with 52.5 m cored and 53.2 m recovered (101.3% recovery). The bit cleared the seafloor at 1145L, 3 October and the rotary table at 1330L.

Hole 824C

The ship was moved 50 m east, and an RCB BHA was run to 978.3 mbsl. Hole 824C was spudded at 0927L, 3 October, at 16°26.705′S, 146°45.753′E. We estimated that the mud line was at 1000.3 mbsl. A 9-7/8-in. hole was washed from 0 to 247.6 mbsf, and Cores 133-824C-1R through -19R were taken from 247.6 to 430.8 mbsf, with 183.2 m cored and 3.21 m recovered (1.75% recovery). Metamorphic basement rocks were penetrated at 406.7 mbsf. The bit cleared the seafloor at 2133L, 3 October.

Hole 824D

The ship was moved 25 m south, and an RCB BHA was run to 987.6 mbsf. Hole 824D was spudded at 2233L, 4 October at 16°26.690′S, 146°45.753′E. We estimated that the mud line was at 1001.9 mbsl. A 9-7/8-in. hole was washed from 0.0 to 334.5 mbsf. Cores 133-824D-1R through -10R were taken from 344.5 to 431.0 mbsf, with 96.5 m cored and 1.06 m recovered (1.1% recovery). Basement was penetrated at ~405.4 mbsf. A two-stand short trip to 380.1 mbsf and back down encountered no drag and only 3.0 m of fill at the bottom of the hole. The bit was released with the mechanical bit release and the pipe was pulled to 90.1 mbsf for logging. Logs were run as follows:

1. The induction/sonic/caliper/gamma-ray (DITE/SDT/NGT/MCDG) logging tool was placed into the hole at 2233L, 5 October and found bottom 19.5 m above the total depth of the hole.

The MBR cleared the seafloor at 0225L, 6 October, and cleared the rotary table at 0425L. The beacon was recalled and recovered.

Table 1 contains the coring summary for Site 824.

SITE GEOPHYSICS

JOIDES Resolution separated from the beacon at Hole 823C at 1830 hr LT (JD 273/0830 UTC) on 30 September 1990, and commenced the 5.5-hr transit to Site 824 (proposed Site NEA-6) at 2342L (JD 273/1342 UTC). A magnetometer was towed immediately after departure, and continuous bathymetric and magnetic data were recorded during the Line 9 transit heading ~80° across the Queensland Trough to the western margin of the Queensland Plateau. The ship arrived at a position of 16°26.702′S and 147°38.000′west of Site 824, at 0454L (JD 273/1854 UTC) on 1 October 1990, ready to start the site location survey.

Site 824 lies in ~1000 m of water on the upper slope of the eastern margin of the Queensland Trough, ~13 km west of the Holmes Reef platform (Fig. 3). It is ~106 km east of Site 823, near the center of the Queensland Trough, and ~43 km west of Site 811, which lies to the east of Holmes Reef. Site 824 forms part of the transect of Leg 133 drilling sites that extends east from the Great Barrier Reef across the Queensland Trough to the western Queensland Plateau in the vicinity of Holmes Reef. The site was selected to understand slope processes in an exclusively carbonate system; to determine the age of the reefal platform and the significance of sea level, oceanographic, and climatic controls on its development; and to determine the nature of Queensland Plateau basement.

The area was first recognized as a potential ODP drilling target on 1971 and 1985 BMR sparker lines (Lines 14/010 and 51/016-017; Fig. 3). In 1987, the BMR vessel, *Rig Seismic*, was used to conduct a site survey at this location (Symonds and Davies, 1988; Feary et al., 1990) and ~40 km of 24-channel, 80-in.^{3} water-gun seismic, magnetic, and bathymetric data were collected on intersecting north-south and east-west lines (BMR Lines 75/39 and 40; Figs. 3 and 4, "Site 823" chapter, this volume). The proposed site lies at the intersection of two lines within this network (Feary et al., 1990), both located using transit satellite/dead-reckoning (DR) navigation.

An important requirement of the Leg 133 site location surveys was that the seismic records obtained on the *JOIDES Resolution* be as close as possible in appearance to those collected during the 1987 site surveys by BMR's *Rig Seismic*, thus reducing ambiguity in site definition and in comparison of the seismic stratigraphy between the two data sets. Accordingly, some modifications were made to the *JOIDES Resolution* seismic deployment systems.

The site location survey was designed to confirm the seismic character and position of Site 824 along the east-west *Rig Seismic* line across it. Following the survey, the site would be relocated using the confirmed global positioning system (GPS) coordinates, and a beacon dropped while maneuvering onto the location using the *Resolution*'s dynamic positioning system. The distribution of regional seismic data in the area around the site is shown in Figure 3, and the tracks of the original *Rig Seismic* site survey and the *JOIDES Resolution* site location survey are shown in Figure 4. Following a reduction in ship speed to 5 kt, the *JOIDES Resolu-*

Table 1. Coring summary, Site 824.

Core no.	Date (Oct. 1990)	Time (UTC)	Depth (mbsf)	Length cored (m)	Length recovered (m)	Recovery (%)
Hole 824A						
1H	1	0335	50.0–59.5	9.5	9.63	101.0
2H	1	0420	59.5–69.0	9.5	9.83	103.0
3H	1	0450	69.0–78.5	9.5	9.72	102.0
4H	1	0515	78.5–88.0	9.5	6.66	70.1
5H	1	0545	88.0–97.5	9.5	9.61	101.0
6H	1	0610	97.5–107.0	9.5	9.68	102.0
7H	1	0635	107.0–116.5	9.5	10.06	105.9
8H	1	0705	116.5–126.0	9.5	9.77	103.0
9H	1	0815	126.0–135.5	9.5	9.49	99.9
10H	1	0915	135.5–137.9	2.4	2.44	101.0
11X	1	1045	137.9–146.4	8.5	0.10	1.2
12X	1	1130	146.4–156.1	9.7	0.00	0.0
13X	1	1210	156.1–165.7	9.6	0.00	0.0
14H	1	1245	165.7–175.2	9.5	9.54	100.0
15H	1	1310	175.2–184.7	9.5	8.88	93.5
16X	1	1415	184.7–194.0	9.3	0.00	0.0
17X	1	1435	194.0–203.6	9.6	5.06	52.7
18X	1	1500	203.6–213.3	9.7	0.00	0.0
19X	1	1520	213.3–223.0	9.7	9.37	96.6
20X	1	1540	223.0–232.7	9.7	0.00	0.0
21X	1	1600	232.7–242.3	9.6	4.87	50.7
22X	1	1620	242.3–252.0	9.7	3.20	33.0
23X	1	1650	252.0–261.6	9.6	0.00	0.0
24X	1	1740	261.6–271.3	9.7	0.18	1.9
25X	1	1810	271.3–281.0	9.7	0.00	0.0
26X	1	1845	281.0–290.6	9.6	0.00	0.0
27X	1	1925	290.6–300.2	9.6	0.00	0.0
28X	1	2105	300.2–309.9	9.7	0.13	1.3
29X	1	2205	309.9–319.5	9.6	0.20	2.1
30X	1	2305	319.5–329.2	9.7	0.18	1.9
31X	2	0001	329.2–338.7	9.5	0.00	0.0
32X	2	0040	338.7–348.4	9.7	0.48	5.0
33X	2	0120	348.4–358.1	9.7	0.00	0.0
34X	2	0225	358.1–367.7	9.6	0.00	0.0
35X	2	0330	367.7–370.2	2.5	0.14	5.6
36X	2	1505	370.2–377.3	7.1	0.47	6.6
			Coring totals	327.3	129.69	39.6
Hole 824B						
1H	2	2345	0.0–5.0	5.0	5.00	100.0
2H	3	0001	5.0–14.5	9.5	9.91	104.0
3H	3	0020	14.5–24.0	9.5	9.82	103.0
4H	3	0035	24.0–33.5	9.5	9.79	103.0
5H	3	0055	33.5–43.0	9.5	9.36	98.5
6H	3	0110	43.0–52.5	9.5	9.41	99.0
			Coring totals	52.5	53.29	101.5
Hole 824C						
1R	3	1500	247.6–257.2	9.6	0.09	0.9
2R	3	1545	257.2–266.8	9.6	0.14	1.5
3R	3	1630	266.8–276.5	9.7	0.00	0.0
4R	3	1715	276.5–286.2	9.7	0.00	0.0
5R	3	1800	286.2–295.8	9.6	0.04	0.4
6R	3	1840	295.8–305.4	9.6	0.07	0.7
7R	3	1930	305.4–315.1	9.7	0.13	1.3
8R	3	2025	315.1–324.8	9.7	0.88	9.1
9R	3	2105	324.8–334.5	9.7	0.00	0.0
10R	3	2150	334.5–344.0	9.5	0.00	0.0
11R	3	2235	344.0–353.6	9.6	0.11	1.1
12R	3	2320	353.6–363.3	9.7	0.00	0.0
13R	4	0015	363.6–372.9	9.6	0.00	0.0
14R	4	0105	372.9–382.5	9.6	0.00	0.0
15R	4	0205	382.5–392.2	9.7	0.00	0.0
16R	4	0310	392.2–401.9	9.7	0.00	0.0
17R	4	0445	401.9–411.5	9.6	0.43	4.5
18R	4	0655	411.5–421.2	9.7	1.00	10.3
19R	4	0855	421.2–430.8	9.6	0.31	3.2
			Coring totals	183.2	3.20	1.7
Hole 824D						
1R	4	1930	334.5–344.0	9.5	0.00	0.0
2R	4	2025	344.0–353.6	9.6	0.00	0.0
3R	4	2120	353.6–363.3	9.7	0.00	0.0
4R	4	2205	372.9–372.9	9.6	0.00	0.0
5R	4	2255	372.9–382.5	9.6	0.00	0.0
6R	4	2345	382.5–392.1	9.6	0.00	0.0
7R	5	0040	392.1–401.8	9.7	0.00	0.0
8R	5	0140	401.8–411.5	9.7	0.03	0.3
9R	5	0445	411.5–421.2	9.7	0.62	6.4
10R	5	0730	421.2–431.0	9.8	0.41	4.2
			Coring totals	96.5	1.06	1.1

Note that all times are given in Universal Time Coordinated or UTC, which is 10 hr later than local time or L.

tion's single channel seismic profiling system was deployed and seismic recording commenced at JD 273/1918 UTC on 30 September 1990 in rough seas (Beaufort Scale force of 4 to 5), with 2- to 3-m swells. The *JOIDES Resolution* sailed east across Site 824 (Fig. 4), when we stopped acquiring seismic dat and retrieved our equipment at JD 273/2056UTC, 30 September 1990, after recording about 12 km of seismic data. No magnetic data were recorded during the site location survey because of a fault in the magnetometer's hardware, which developed during the transit to the Site 824 area. GPS navigation was used throughout the survey, and we consider the ship's track to be accurately positioned. A new streamer, which was configured in exactly the same manner as the old one used previously, was deployed duirng this survey and appeared to operate well. Synchronization problems between the two 80-in.^{3} water guns, probably related to a defective blast phone, developed at about JD 273/1939UTC and resulted in substantial reduction of data quality. This improved after JD 273/2011UTC, when the port gun was turned off. In general, fair quality analog monitor records were obtained (Fig. 5), although they are noisy because ofthe relatively rough seas. At the site, reasonable correlation existed between *Rig Seismic* and *JOIDES Resolution* seismic profiles (Fig. 5); however, because of the compressed nature of the *Resolution*'s seismic records and the absence of definitive seismic characteristics, reliable confirmation using only seismic data was difficult. The final site location (as marked on the GPS-navigated *JOIDES Resolution* seismic profile) may be a little east of that proposed in the *Rig Seismic* data (Fig. 5).

Following the survey, *JOIDES Resolution* returned to the confirmed GPS position of Site 824 at JD 273/2130UTC on 30 September 1990. The thrusters were lowered and final positioning of the ship over the site was achieved using dynamic positioning. A beacon was dropped at JD 273/2206UTC; final coordinates of Hole 824A are 16°26.704′S and 147°45.737′E, in a water depth of 1000.4 m (drill-pipe measurement from sea level).

A planated basement surface is clearly visible at about 0.4 s TWT (two-way traveltime) below the seafloor in both the *JOIDES Resolution* and *Rig Seismic* water-gun data across the site (Fig. 5). The sedimentary section at Site 824 can be broadly divided into three main seismic units. The upper unit is about 0.19 s TWT (~180 m) thick, and contains both subparallel, discontinuous, and chaotic reflection configurations. It onlaps the underlying 0.11s TWT (~100 m) thick unit, which contains similar reflection patterns, as well as reflection-free zones. This unit also onlaps the underlying unit, which sits on basement. The basal unit is about 0.11 s TWT (~100 m) thick at the site, but thickens significantly to the east toward the Holmes Reef bank. This unit contains irregular, disrupted, and chaotic reflector configurations and becomes

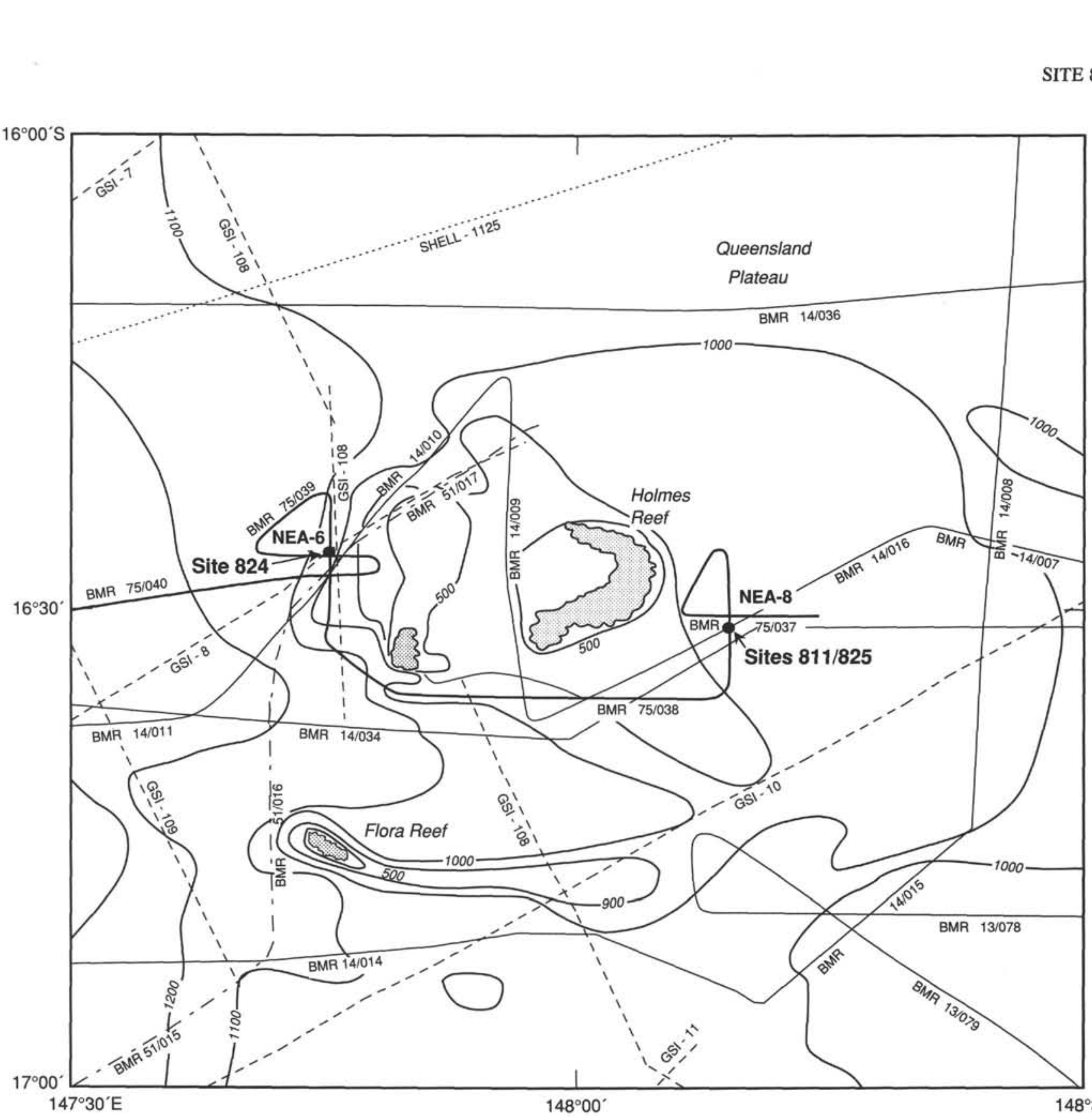

Figure 3. Track chart showing the distribution of regional seismic data in the area around Site 824. Also shows the location of Sites 811/825, and the simplified bathymetry in meters.

more reflection-free toward the bank; it has the form of a carbonate-platform debris apron. "Basement" at the site has a smooth, planated surface and exhibits very little reflection character.

To provide some predictive capability during the drilling at Site 824, an estimate of the two-way traveltime (TWT)/depth relationship below the seafloor was made using stacking derived interval velocities from the BMR site survey seismic lines across the site (Fig. 6).

LITHOSTRATIGRAPHY

Introduction

Site 824 is located on the western slope of the Queensland Plateau, 13 km west of Holmes Reef. Four holes were drilled at Site 824 in 1001 m of water depth and penetrated a composite sedimentary sequence consisting of 430 m of periplatform, pelagic, and shallow-water carbonates. Site 824 bottomed into the metamorphic continental basement of the Queensland Plateau. Sediments were washed down to 50 mbsf in Hole 824A and then APC and XCB cored to a total depth of 377.3 mbsf with an average recovery of 39.6%. The upper 52.5 m of the sedimentary column was fully recovered in Hole 824B by APC (average recovery 101.5%). In Hole 824C, the upper 247.6 m of the sedimentary column was washed, and then cored to 430.8 mbsf using the RCB, with poor recovery that averaged only 1.7%. In Hole 824D, the upper 344.5 m of the sedimentary column was washed and then RCB cored to 431.0 mbsf, with little recovery.

Sediments recovered at Site 824 consist mostly of pure carbonates that were deposited either as (1) a mixture of pelagic carbonates (planktonic foraminifers and coccoliths) and bank-derived fine particles (micrite), defined by Schlager and James (1978) as periplatform sediments, recovered as oozes and chalks according to their diagenetic state, or (2) redeposited layers of bank-derived packstone and rudstone

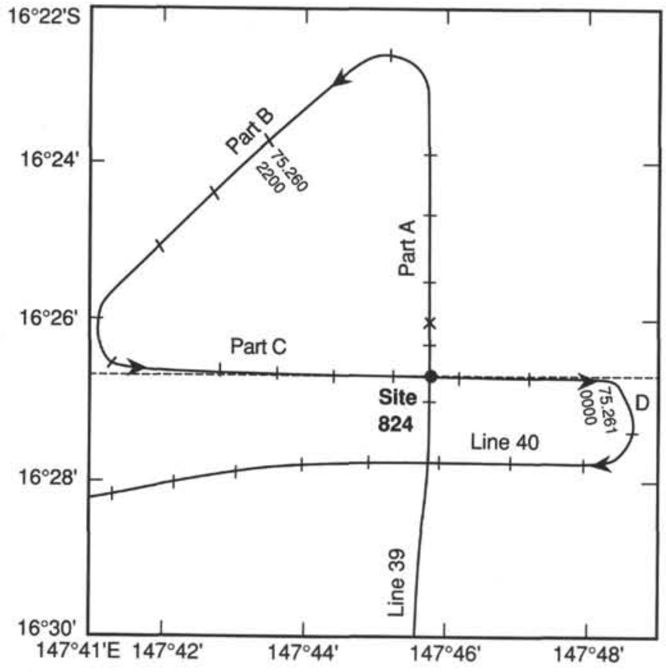

Figure 4. *JOIDES Resolution* Leg 133 site location tracks (dotted line) and *Rig Seismic* 1987 site survey tracks (solid line) around Site 824.

sediments, deposited by gravity flows (calciturbidites), debris flows, and possibly grain flows. Most of the coarse sand grains and gravels in the redeposited packstones and rudstones and in the lower part of Site 824 were identified as fragments of mollusks (bivalves and gastropods), bryozoans, corals (massive and branching) and corallinacean algae (encrusting, branching, or rhodoliths).

The upper 340-m in Site 824 was divided into five lithologic units (Units I–V) on the basis of the variable proportions between periplatform sediments and discrete layers or intervals of redeposited bank-derived coarse grained particles. Subunits were defined in order to identify more homogeneous lithologic intervals within a given unit. The general lithologies of the lower 90-m of Site 824 were quite different from the upper 340-m and were subdivided into two units. Unit VI consists of a bioclastic rudstone distinguished from the overlying lithologies by its assemblage of larger foraminifers, mollusks, bryozoans, and corallinacean algae (foramol). The lowest part of Site 824, Unit VII, comprises partially weathered metasediments of the Queensland Plateau basement.

Lithologic Units

A summary of the Site 824 lithologic units appears in Figure 7.

Unit I (Cores 133-824B-1H through -6H and Core 133-824A-1H through Section 133-824A-5H-6, 150 cm; depth, 0–105 mbsf; age, Pleistocene)

Unit I is characterized by discrete layers and intervals of redeposited bioclastic packstone and rudstone separated by intervening periplatform oozes and chalks, that consist of a mixture of 40%–60% fine bank-derived aragonite particles (micrite) identified by X-ray diffraction (see "Inorganic Geochemistry" section, this chapter) and variable proportions of planktonic particles, nannofossils, foraminifers, and in the upper few meters of Site 824, pteropod tests. Unit I consists of two major 45- to 50-m-thick upward-fining packages. The lower part of each package consists of a thick homogeneous interval of bioclastic redeposited packstone sediments (Subunits IB and ID), whereas the upper part of each package consists of alternating thin layers of bioclastic redeposited sediments and discrete intervals of periplatform oozes and chalks (Subunits IA and IC).

Subunit IA (Sections 133-824B-1H-1 through -4H-2; depth, 0–27 mbsf; age, Pleistocene)

Subunit 1A is characterized by intervals of white periplatform oozes and chalks, ranging in thickness from 20 to 60 cm and intervening between numerous bioclastic layers. The periplatform sediments, unlithified in the upper part of Subunit IA, quickly become firmer with increasing core depth. Chalky horizons already occur within the lower part of Core 133-824B-2H. The periplatform intervals separate numerous layers of very pale brown bioclastic packstone sediments. Size fraction of the bioclastic particles within the discrete layers increases downward in Subunit IA from fine to medium sand. The thickness of the redeposited layers, ranging from 10 to 20 cm to a maximum of 85 cm, remain rather constant throughout Subunit IA.

Subunit IB (Section 133-824B-4H-2 to Core 133-824B-6H; depth, 27–52 mbsf; age, Pleistocene)

Subunit IB consists mostly of bioclastic packstone redeposited sediments with foraminifers, nannofossils, and micrite. Grain size variations show a coarsening upward trend from very fine sand-sized bioclastic grains in Core 133-824B-6H to very coarse sand-sized grains in Core 133-824B-5H and, finally, to silt and gravel sized grains in Core 133-824B-4H. Several distinct graded beds up to 3-m in thickness are distinguished in Subunit IB, although most of the packstone sediments are homogeneous and without clear layers. Only a few thin layers of periplatform ooze (bioclastic micritic mudstone), in Sections 133-824B-6H-1 and -2, separate the redeposited bioclastic packstone sediments within Subunit IB. Degree of lithification, ranging from unlithified to partially lithified packstones, is variable throughout Subunit IB.

Subunit IC (Sections 133-824A-1H-1 through -2H-6; depth, 52–68 mbsf; age, Pleistocene)

The lithologies in Subunit IC resemble the ones described in Subunit IA. Subunit IC consists of numerous 5- to 145-cm-thick (average 60 cm) layers of bioclastic redeposited packstone sediments separated from one another by 20- to 40-cm-thick intervals of periplatform oozes and chalks.

Subunit ID (Core 133-824A-3H through Section 133-824A-5H-6; depth, 68–105 mbsf; age, Pleistocene)

Subunit ID consists of homogeneous, white, unlithified bioclastic redeposited packstone sediments with abundant fragments of *Halimeda* and bryozoans. Individual beds cannot easily be distinguished with the exception of some graded beds in the upper half of Core 133-824A-5H, where the layer thicknesses range from 25 to 110 cm, showing a thinning trend upward. Grain sizes in the upper part of Subunit ID range between fine and medium bioclastic sands, whereas the base of Subunit ID, Section 133-824A-5H-6, consists of very coarse sand, redeposited packstone and rudstone sediments containing coral rubble.

Unit II (Section 133-824A-5H-6 to Core 133-824A-9H; depth, 105–135.5 mbsf; age, late Pliocene)

Unit II consists of numerous discrete layers of redeposited bioclastic packstone separated by intervening periplatform oozes and chalks, that consist of a mixture of up to 40% fine bank-derived aragonite particles (micrite) identified by X-ray diffraction (see "Inorganic Geochemistry" section, this chapter)

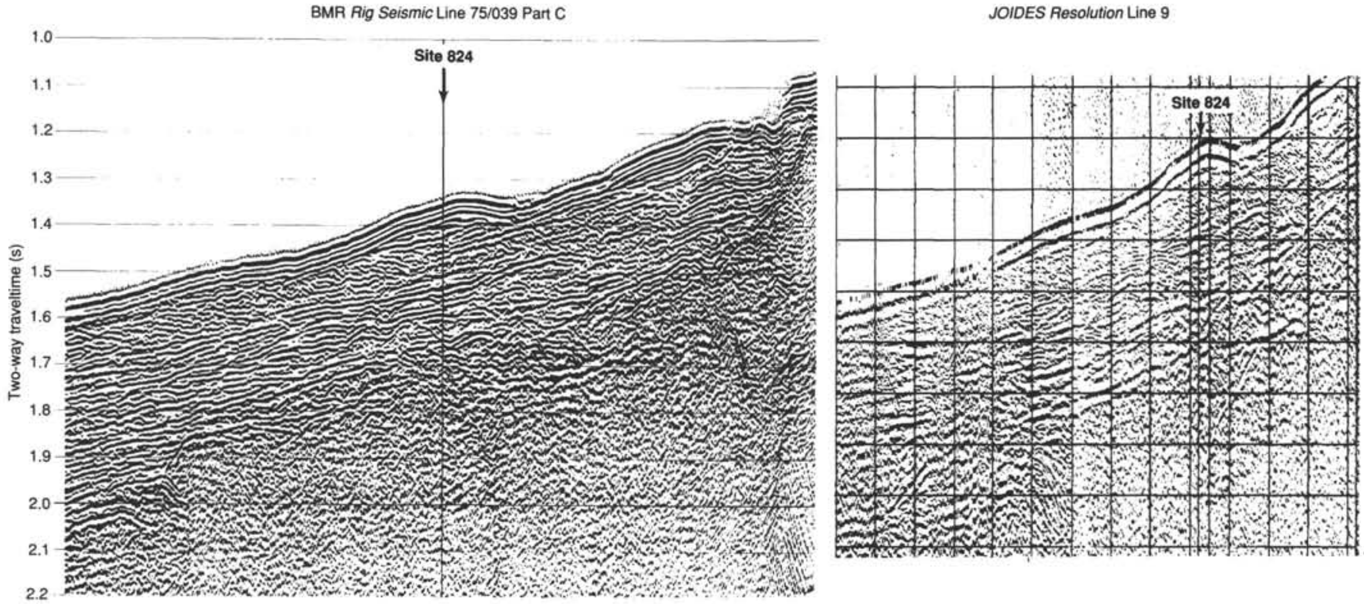

Figure 5. Comparison of *JOIDES Resolution* and *Rig Seismic* 80-in.^{3} water-gun seismic profiles across Site 824.

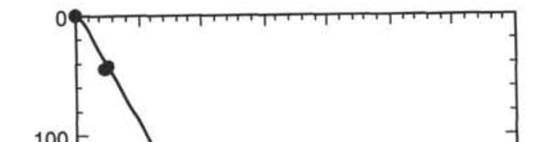

Figure 6. Two-way traveltime/depth curve estimated for Site 824.

and variable proportions of planktonic particles, nannofossils, and foraminifers. Bioclastic grains in the redeposited layers consist of shallow-water carbonate fragments of corals, bryozoans, echinoderms, and mollusks. Frequency of redeposited layers varies within Unit II. Redeposited layers are more numerous in Core 133-824A-8H than in Cores 133-824A-7H and -9H. The redeposited packstone sediment layers vary in thickness and are separated from one another by a minimum of 10- to 20-cm-thick intervening periplatform oozes and chalks.

Unit III (Core 133-824A-10X to Section 133-824A-14H-1; depth, 135.5–166 mbsf; age, Pliocene)

Unit III is defined in a poorly recovered interval of Hole 824A. Sediments were recovered in Sections 133-824A-10X-1 and -2, and in Section 133-824A-14H-1. Unit III consists of white, very pale brown to dark gray, well-cemented, limestone pieces, possibly created by drilling, which contain clasts of bioclastic rudstone and packstone. Allochems consist of large fragments of corals (cm in size), encrusting and branching corallinacean algae as well as complete 3-cm-in-diameter rhodoliths, embedded in a sand-size bioclastic packstone matrix.

Unit IV (Section 133-824A-14H-1 through Core 133-824A-21X; depth, 166–242.3 mbsf; age, middle to late Miocene)

Unit IV consists of very white to light gray nannofossil oozes and chalks with variable proportions of bioclasts and micrite. Aragonite in trace amount is present only in the upper part of Unit IV (see "Inorganic Geochemistry" section, this chapter). Chalks that contain larger amounts of irregular recrystallized grains become calcitic chalk with bioclasts, nannofossils, and micrite. Redeposited packstone layers are more common in Core 133-824A-15X. Layers of fine to medium sand-sized, redeposited carbonate particles are very pale brown in color. Graded bedding is often not observed, although the bases of the redeposited layers are usually more distinct and their tops more gradational. Shallow-water components are abundant, i.e., corals, large foraminifers, coralline algae, alcyonarian spicules, mollusks, and echinoids. The degree of lithification increases with increasing depth in Unit IV. Subunit IVA (Cores 133-824A-14H and -15H) is distinguished from Subunit IVB (Cores 133-824A-15H and -21X) by the occurrence of redeposited packstone layers in Subunit IVA, whereas redeposited layers do not clearly occur in Subunit IVB.

Unit V (Cores 133-824A-21X through -31X and Cores 133-824C-1R through -10R; depth, 242.3–338.7 mbsf; age, middle to late Miocene)

Unit V can be subdivided into two subunits on the basis of the occurrence of planktonic foraminifers and several distinct layers of redeposited sediments in Subunit VA, whereas

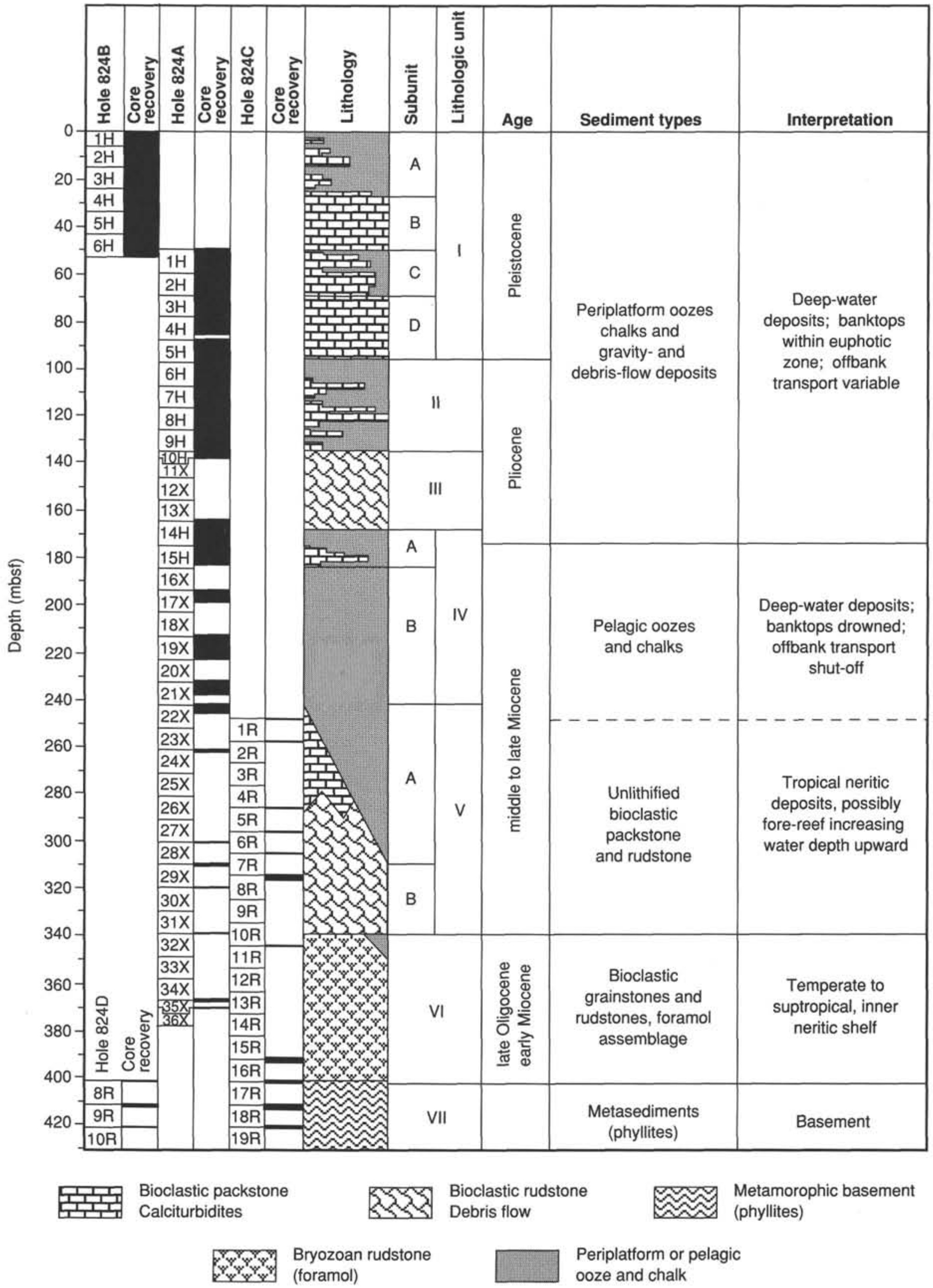

Figure 7. Lithostratigraphy of Site 824.

planktonic foraminifers and layers of clearly redeposited sediments are not observed in Subunit VB.

Subunit VA (Cores 133-824A-22X to the middle of -28X and Cores 133-824C-1R to the middle of -7R; depth, 242.3–309.9 mbsf; middle to late Miocene)

Subunit VA consists of alternating very white, foraminifer (planktonic) chalk and white to very pale brown beds of redeposited, shallow water derived, carbonate grains (mollusks, corals, corallinacean algae, fragments or complete 3-cm-in-diameter rhodoliths with laminar coating, fragments of *Halimeda*? as molds, larger foraminifers (Alveolinidae), small miliolids, and textulariids. Well-rounded, isolated up to 3-cm-in-diameter lithoclasts are also observed embedded in-planktonic foraminifer chalks. It is difficult to interpret the mode of deposition for the redeposited beds due to poor recovery in the lower part of Site 824. A trend toward deepening and more pelagic character of the depositional environments in Subunit VA can be deduced based upon the vertical sediment succession from skeletal and lithoclastic rudstones at the base of Subunit VA to larger foraminifer floatstones with more abundant planktonic foraminifers in the upper part of Subunit VA. Redeposited clasts are densely cemented recrystallized limestones. Coral and mollusk fragments are preserved as molds.

Subunit VB (Cores 133-824A-28X to base of -31X and middle of Core 133-824C-7R to middle of Core 133-824C-10R; depth, 309.9–338.7 mbsf; middle to late MIocene)

Subunit VB consists of white to very pale brown, dense skeletal packstone and rudstone. Most common grains are branching corals, pelecypods, gastropods, echinoids, benthic foraminifers (miliolids and larger foraminifers, i.e., Alveolinidae), encrusting and branching corallinacean algae, and complete rhodoliths. Floatstones with branching corals thinly encrusted by corallinacean algae occur at the base of Subunit VB. Coral and mollusk fragments are preserved as molds throughout Subunit VB. Quartz grains occur at some levels.

Unit VI (Cores 133-824A-32X through -36X and Cores 133-824C-10R through -17R; depth, 338.7–401.9 mbsf; age, Miocene to late Oligocene)

Unit VI consists of very white bioclastic branching bryozoan-rich rudstone with poorly preserved corallinacean algal, mollusk, larger foraminifer, and tiny branching (ahermatipic?) coral fragments. Grain size ranges from sand to granules. In addition angular quartz grains occur throughout Unit V. Carbonate grains are highly recrystallized and tightly cemented, though interparticle porosity is high, giving a chalky appearance to the limestone. The color of the very poorly sorted quartz bioclastic sandstone with muddy matrix at the base of Unit VI ranges from a dark yellowish brown to gray. Identifiable carbonate grains are fragments of bryozoans and larger foraminifers. Quartz grains vary in appearance from milky to clear, in shape from rounded to angular, and reach a 3 mm maximum grain size. Lithoclasts of reworked black phyllite, several mm in diameter, occur within the base of Unit V.

Unit VII (Cores 133-824C-17R through -19R and Cores 133-824C-8R through -10R; depth, 401.9–431 mbsf; age, unknown)

The upper part of Unit VII consists of a deeply weathered, mottled orange and brown regolith, a fine-grained rock with 1-mm-sized quartz grains. Fractures are coated with manganese oxide and dendrites occur in Core 133-824C-17R. The regolith covers black to very dark gray carbonaceous and quartzose, as well as chloritic, phyllites characterized by intense crenulation, kink bands, microfaults, and irregular transverse quartz and calcite veins. Locally quartzitic lenses parallel to the foliation give the rock in Unit VII a conglomeratic appearance. Light gray, finely crystalline metavolcanic rock of possible basic composition is intercalated within the phyllites with common pyrite occurrence at the lithologic contacts.

Interpretation

The different lithologies drilled at Site 824, located on the leeside of the modern carbonate platform of Holmes Reef, have recorded the entire evolution of the northwest corner of the Queensland Plateau since the initial late Oligocene transgression on a metamorphic basement (Unit VII). The oldest (late Oligocene to early Miocene) carbonate (Unit VI) deposited at Site 824, characterized by a temperate or subtropical foraminiferal assemblage, is interpreted to have been deposited in an open shelf environment. The bio-assemblage in the overlying middle Miocene carbonates (Subunit VB) is more tropical in character and is interpreted to correspond to a fore- or back-reef environment. The depth of the depositional environment increased within Unit V. The carbonate sediments deposited within Subunit VA are clearly characteristic of an open marine environment because of the first occurrence of planktonic foraminifers and redeposited shallow carbonate material in numerous calciturbidites and debris-flow deposits. Carbonate grains in the redeposited layers have a clear neritic origin, indicating that Site 824 was within close proximity to a producing carbonate bank (paleo Holmes Reef) during the middle Miocene. Unit IV was deposited, during the middle and late Miocene, in an environment similar to the underlying Subunit VA. However, water depth might have been deeper and the environment of deposition more distal from the producing carbonate bank than during the interval of Unit V deposition. Lack of calciturbidites and the more pelagic character of the chalks (low proportion of bank-derived micrite in the fine fraction) within most of Unit IV indicates that during most of Unit IV the adjacent shallow carbonate platform was not producing and exporting large volumes of neritic carbonate toward the deep surroundings, either because the platform was drowned or exposed. Similar, but more pelagic, sediments characterized by the absence of calciturbidites and fine bank-derived carbonate (aragonite or micrite) were drilled on the Queensland Plateau at Sites 811, 813, 814, and 817 during a similar time interval that included late Miocene and early Pliocene.

Influx of bank-derived material as fine aragonite mixed with the pelagic carbonates (planktonic foraminifers and coccoliths) and as calciturbidites into the deep areas adjacent to the paleo Holmes Reef seems to have resumed during the Pliocene (most probably during the early part of the late Pliocene) (Unit II) starting with the deposition of a 30-m-thick package of debris flows with abundant coral and algal (corallinacean) fragments (Unit III). Production and input of bank-derived carbonate from Holmes Reef seems to have varied through the Pleistocene (Unit I) on the basis of the variable proportion in Unit I of bank-derived fine aragonite and the calciturbidite bundling.

BIOSTRATIGRAPHY

Introduction

Four holes were drilled at Site 824. Nannofossils, planktonic foraminifers, and benthic foraminifers were examined from core-catcher samples at Holes 824A and 824B. The biostratigraphic results indicate a Pleistocene section in Hole 824B, and the record in Hole 824A ranges from Pleistocene to lowest Miocene–uppermost Oligocene (combined planktonic foraminifer zone N3–N4; Fig. 8). There are few reliable datum

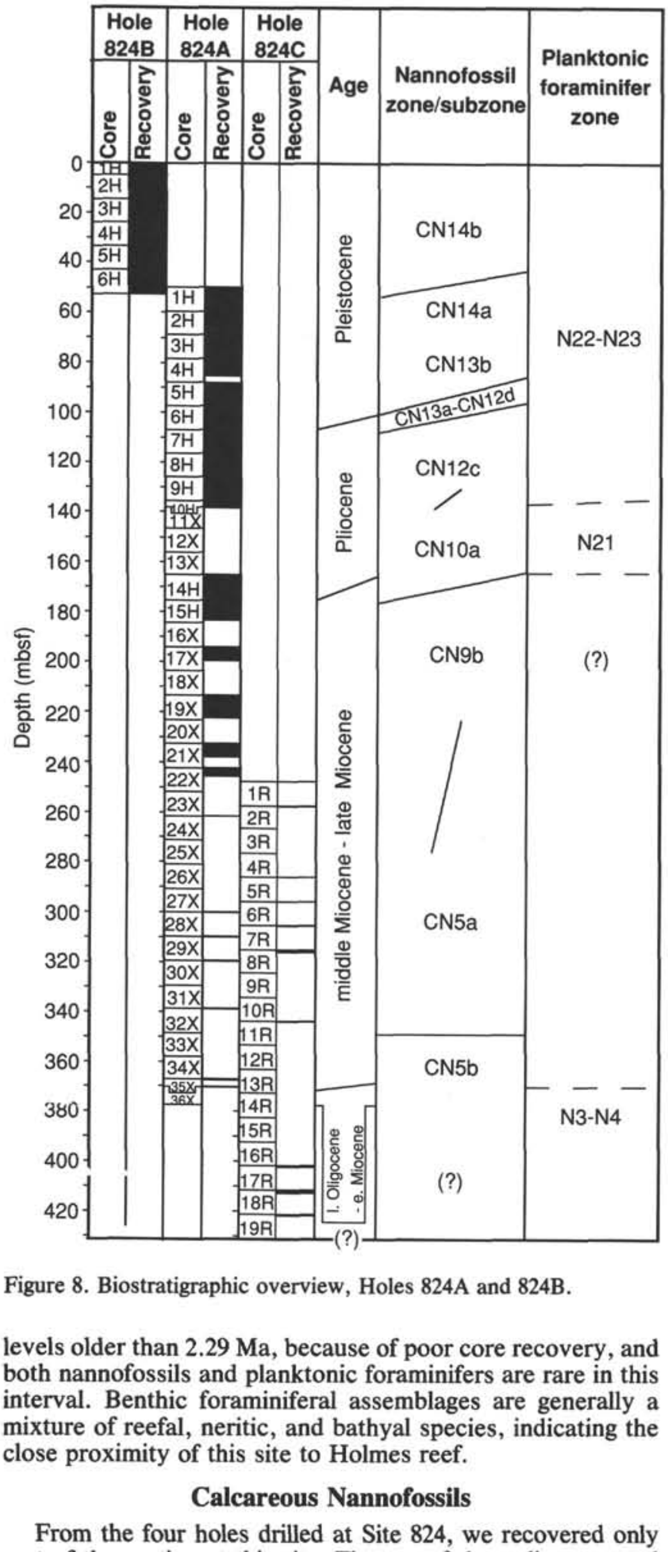

Figure 8. Biostratigraphic overview, Holes 824A and 824B.

levels older than 2.29 Ma, because of poor core recovery, and both nannofossils and planktonic foraminifers are rare in this interval. Benthic foraminiferal assemblages are generally a mixture of reefal, neritic, and bathyal species, indicating the close proximity of this site to Holmes reef.

Calcareous Nannofossils

From the four holes drilled at Site 824, we recovered only part of the section at this site. The age of the sediment cored extends from the late Pleistocene (possibly Holocene) at the top to probably middle Miocene at 348.4 mbsf, the lowest level at which sediments can be dated by nannofossils. Considering the time span covered, the number of biohorizons that can be reliably determined is very small, owing to sporadically poor core recovery, poor nannofossil recovery in unfavorable lithology (environmental exclusion), and poor preservation or absence of marker species. Following is a summary of the biostratigraphy of this site (based on recovery in Holes 824A and 824B), from the top of the section downward.

The youngest biohorizon is the highest occurrence of *Pseudoemiliania lacunosa* (0.465 Ma) in Sample 133-824B-6H-CC (43.0–52.5 mbsf). This is the only biohorizon identified in Hole 824B; all others were identified in Hole 824A. The first of these is the highest occurrence of *Calcidiscus tropicus* (1.48 Ma) in Sample 133-824A-5H-CC (88.0–97.5 mbsf). Although there is complete core recovery between the last two biohorizons, no intervening datums were recognized owing to unfavorable lithology and poor preservation. The next lower core, Sample 133-824A-6H-CC (97.5–107.0 mbsf), marks the highest occurrence of *Discoaster pentaradistus* (2.29 Ma). From this level downward to Sample 133-824A-14H-CC reliable biohorizon determinations could not be made, but in Sample 133-824A-14H-CC (165.7–175.2 mbsf), five-rayed, symmetrical asteroliths are abundant, and these are probably heavily calcified *Discoaster quinqueramus*. However, this may not be the highest occurrence of this species, because the two preceding cores had no recovery. Therefore, the 5.26 Ma age of the highest occurrence of *Discoaster quinqueramus* should be viewed as a minimum age. The several Pliocene biohorizons between the *Discoaster quinqueramus* highest occurrence, which clearly marks this level as upper Miocene, and the next datum above, the late Pliocene *Discoaster pentaradiatus* highest occurrence, are not identifiable in the core-catcher samples.

One additional datum may be indicated by the data, and that is the highest occurrence of *Cyclicargolithus floridanus* (11.0 Ma) in Sample 133-824A-32X-CC (338.7–348.4 mbsf). No datable nannofossil assemblages were recovered below 348.4 mbsf.

Planktonic Foraminifers

The uppermost three cores of Hole 824B (133-824B-1H-CC through -3H-CC) contain abundant, well preserved planktonic foraminifers. The presence of abundant *Globigerinoides ruber* pink in Sample 133-824B-1H-CC indicates an age of older than 0.12 Ma. Samples 133-824B-2H-CC and -3H-CC yield abundant *Globorotalia truncatulinoides*, and therefore this interval can be assigned to Zone N22–N23. Samples 133-824B-4H-CC through -6H-CC contain rare planktonic foraminifers, and no age-diagnostic species are present.

Planktonic foraminifers recovered from Hole 824A are generally sparse and poorly preserved, except for Samples 133-824A-6H-CC, -7H-CC, and -14H-CC. An interval of poor recovery having no planktonic foraminifers ranges from Samples 133-824A-23X-CC through -34X-CC. The highest occurrence of *Globigerinoides fistulosus* (1.6 Ma) is present in Sample 133-824A-6H-CC. The lowest occurrence of *Globorotalia truncatulinoides* is in Sample 133-824A-8H-CC; therefore, the boundary between combined Zones N22–N23 and N21 is somewhere in Sample 133-824A-9H-CC. Sample 133-824A-14H-CC contains abundant late Pliocene foraminifers such as *Globigerinoides obliquus, Neogloboquadrina acostaensis, Globoquadrina altispira, Sphaeroidinellopsis seminulina,* and *Globorotalia tumida plesiotumida*. This sample is older than 3.0 Ma based on the latest occurrence of *S. seminulina,* and younger than 3.9 Ma based on the absence of *Globigerina nepenthes*. Sample 133-824A-36X-CC yields sparse specimens of *Globigerina ciperoensis, Globigerina praebulloides,* and *Globorotalia kugleri,* which refers this sample to Zones N3–N4 with an age range of 21.8–23.7 Ma (latest Oligocene to earliest Miocene).

Benthic Foraminifers

Benthic foraminifers from Site 824 show poor to moderate preservation with some recrystallization. Core-catcher samples contain mixtures of reefal, neritic, and bathyal benthic foraminifers, indicating the downslope transport and mixing of benthic foraminiferal faunas. Reefal benthic foraminifers found in Site 824 core-catcher samples are *Amphistegina* spp. and *Asterigerina* spp. Taxa typical of the neritic zone include *Buliminella elegantissima, Discorbis* spp., *Elphidium* spp., and *Planorbulina* sp. Scattered occurrences of benthic foraminifers that are generally found together in the bathyal zone include *Bulimina mexicana, Cibicidoides bradyi, Cibicidoides pachyderma, Hanzawaia mantaensis, Hyalinea balthica, Hoeglundina elegans, Laticarinina pauperata, Planulina wuellerstorfi, Plectofrondicularia parri, Pyrgo murrhina, Sphaeroidina bulloides, Uvigerina auberiana, Uvigerina hispida,* and *Uvigerina proboscidea* (van Morkhoven et al., 1986).

PALEOMAGNETISM

Paleomagnetic measurements at Site 824 included a composite from Holes 824A (50.0–377.3 mbsf) and 824B (0.0–52.5 mbsf). The recovered cores were measured at NRM and 15 mT AF steps on a 10 cm measurement interval. Shipboard data failed to resolve a magnetic reversal stratigraphy, which with the biostratigraphic markers, might be used to provide refined age-dating. The absence of reliable reversal stratigraphy is probably related to the weak remanence, high water content, possible disturbance from drilling and core processing, and the occurrence of large shallow-water-derived clasts. The combination of these factors results in a scattered inclination record and in uncertain polarities (Fig. 9).

The NRM and AF 15-mT intensities are highly variable (10^{-1}–10 mA/m) throughout the recovered sections, often showing high intensity spikes at the core tops. After 15-mT AF demagnetization, intensity decreases more than 50% from ~0.11 to ~0.04 mA/m. This response to AF demagnetization suggests small concentrations of a magnetite remanence carrier. Volume magnetic susceptibility throughout much of the holes is very weak (~2–2 × 10^{-6} cgs) except for the top 1-m of Hole 824B and an interval between 58 and 75 mbsf in Hole 824A.

A total of 141 discrete samples were collected from Site 824 to assess whether a reversal stratigraphy can be extracted in a land-based shielded laboratory.

SEDIMENTATION RATES

Sediments recovered from holes drilled at Site 824 yielded a rather uneven biostratigraphy, owing in part to poor recovery, but probably even more to poor preservation and, perhaps, to environmental exclusion of key marker species. Moreover, the few biohorizons recognized may not be accurately placed for the above reasons. The sediment section with usable biostratigraphic control extends from the late Pleistocene to middle Miocene. The sedimentation rate, plotted on the age/depth curve (Fig. 10), does not seem to be exceptionally irregular, even though the biohorizons on which it is based may not be particularly accurate.

The youngest identified biohorizon, the highest occurrence of *Pseudoemiliania lacunosa* (0.465 Ma), is in Sample 133-824B-6H-CC and is assigned a depth to the midpoint of that core of 47.8 mbsf. Assuming a Holocene age at the seafloor, the sedimentation rate for the latest Pleistocene–Holocene is ~10 cm/k.y. The next biohorizon is the early Pleistocene highest occurrence of *Calcidiscus tropicus* (1.48 Ma) in Sample 133-824A-5H-CC (88.0–97.5 mbsf), and the sedimentation rate between this and the last previous biohorizon is about 5 cm/k.y. The rate decreases further to 1.2 cm/k.y. from the *Calcidiscus tropicus* highest occurrence to the late Pliocene *Discoaster pentaradiatus* highest occurrence (2.29 Ma) in the next lower core, Sample 133-824A-6H-CC (97.5–107.0 mbsf). From this to the next identified biohorizon, the uppermost

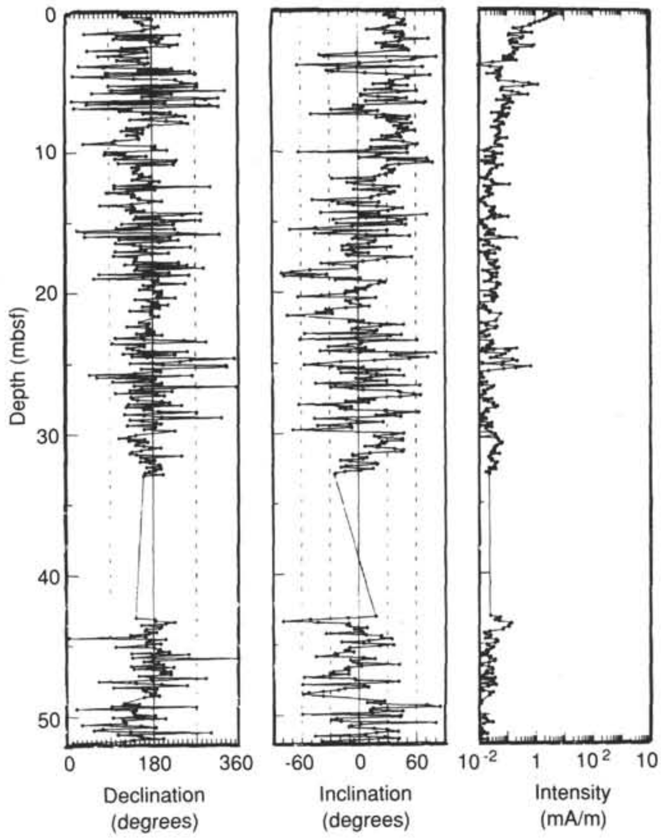

Figure 9. Representative plot of scattered inclination values measured in Hole 824B after 15 mT AF demagnetization.

Miocene highest occurrence of *Discoaster quinqueramus* (5.26 Ma) in Sample 133-824A-14H-CC (165.7–175.2 mbsf), the sedimentation rate roughly doubles to 2.2 cm/k.y. For the last segment, which extends to the highest occurrence of *Cyclicargolithus floridanus* (11.0 Ma) in Sample 133-824A-32X-CC (338.7–348.4 mbsf), the rate is higher again, at about 3 cm/k.y. However, the precision of these numbers should not be overestimated, because the biostratigraphy at this site is relatively crude compared to most of the other sites cored during this leg.

INORGANIC GEOCHEMISTRY

Interstitial Waters

Calcium, Magnesium, and Strontium

Interstitial water samples were taken from Cores 133-824A-1H, -2H, -3H, -5H, -8H, -14H, -17X, -21X, -29X, and Cores 133-824B-1H, -2H, -3H, -4H, -6H. Samples were squeezed and analyzed according to the methods outlined in the "Explanatory Notes" chapter (this volume).

Values for calcium show a small decrease from seawater values of 10.44 to 10.06 at 12.45 mbsf (Table 2 and Fig. 11). Below this depth, calcium concentrations increase to 10.79 mM by 235.60 mbsf. Magnesium concentrations show little change from seawater concentrations of 54.87 mM in the top 75 mbsf of Site 824. Below this depth magnesium concentrations decrease slightly to 53.97 mM at 50.45 mbsf. With increasing depth, concentrations rise to 55.68 mM at the bottom of the sampled interval (Table 2 and Fig. 11). The consistency of the magnesium and calcium profiles may be the result of either contamination by modern seawater in the

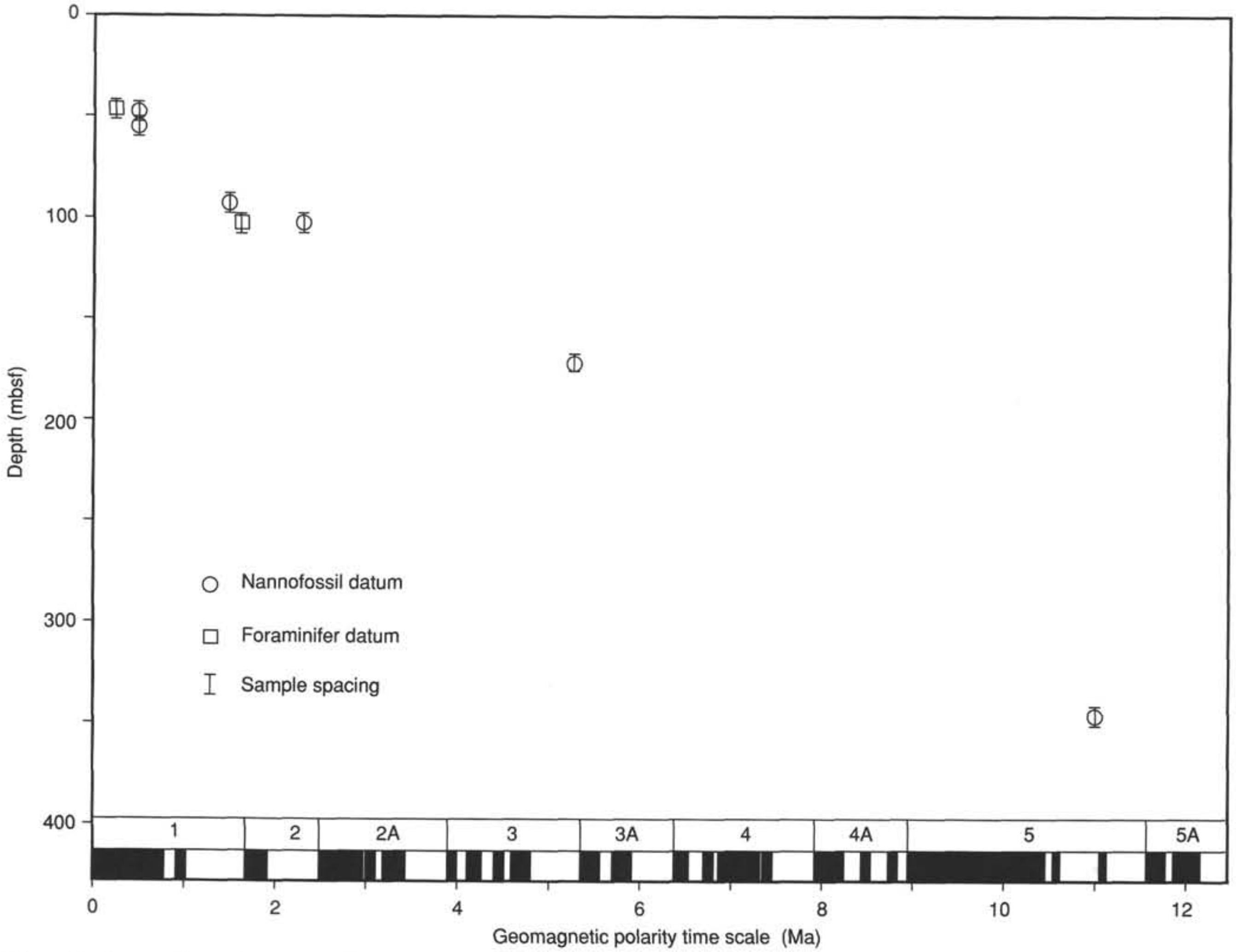

Figure 10. Age vs. depth plot for Site 824.

Table 2. Interstitial water data for Site 824.

Core, section, interval (cm)	Depth (mbsf)	pH	Alkalinity (g/kg)	Salinity (mM)	Chloride (mM)	Magnesium (mM)	Calcium (mM)	Sulfate (mM)	Ammonia (μM)	Silica (μM)	Potassium (mM)	Strontium (μM)
Seawater	0.00	7.99	2.745	35.2	556.43	54.87	10.44	29.41	71	4	10.30	110
133-824B-												
1H-2, 145–150	2.95	7.62	3.650	35.0	540.97	54.12	10.30	29.19	14	109	12.17	203
2H-5, 145–150	12.45	7.37	3.406	35.5	540.97	54.72	10.06	29.62	45	95	10.81	323
3H-5, 145–150	21.95	7.40	3.388	35.2	541.94	54.16	10.30	29.67	34	93	10.43	326
4H-5, 145–150	31.45	7.60	2.994	35.2	541.94	54.11	10.26	29.73	79	91	10.17	249
5H-5, 145–150	40.95	7.58	3.066	35.2	540.97	54.29	10.37	29.20	34	89	11.68	285
6H-5, 145–150	50.45	7.41	3.064	35.2	539.04	53.97	10.45	29.00	21	91	10.35	208
133-824A-												
1H-5, 140–150	57.40	7.57	3.339	35.0	547.73	54.19	10.47	29.52	27	91	11.48	277
2H-5, 140–150	66.90	7.35	3.037	35.0	545.80	54.81	10.50	28.97	19	97	10.71	271
3H-4, 140–150	74.90	7.29	3.375	35.0	540.97	54.29	10.46	30.00	16	91	9.85	270
5H-5, 140–150	95.40	7.69	2.906	35.0	540.97	53.23	10.49	29.89	19	85	10.11	265
8H-2, 140–150	119.40	7.62	3.100	35.0	545.80	53.83	10.67	29.38	38	93	10.26	280
14H-5, 140–150	173.10	7.52	2.973	35.0	550.63	54.45	10.74	29.63	34	131	11.07	223
17X-2, 145–150	195.95	7.63	3.106	35.8	556.43	55.58	10.74	30.47	19	212	11.89	212
21X-2, 140–150	235.60	7.65	3.062	35.8	560.29	55.68	10.79	29.96	16	196	11.30	234

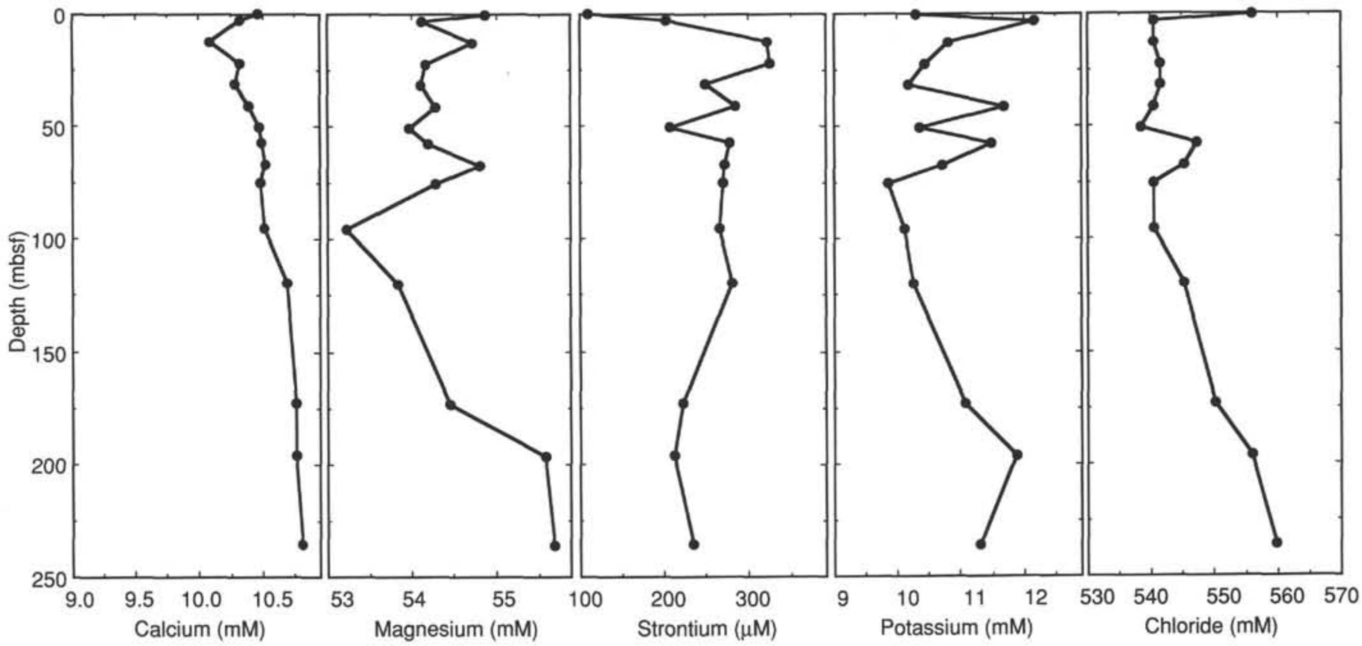

Figure 11. Calcium, magnesium, strontium, potassium, and chloride data as a function of depth for Site 824.

samples due to the sandy nature of the sediment, or to fluid flow in the porewaters as may have been seen at Sites 811, 812, 813, and 814.

Strontium concentrations increase from a seawater value of 110 μM to 326 μM at 21.95 mbsf. Below this depth values gradually decrease to 234 μM at the bottom of the sampled interval (Table 2 and Fig. 11). The small increase in strontium near the top of the hole results from dissolution of aragonite and precipitation of calcite. Potassium concentrations fluctuate around 11 mM for the entire sampled interval at Site 824 (Table 2 and Fig. 11). The consistency of the potassium concentrations reflects the lack of clay mineral diagenesis in the sediments.

Chloride

Chloride concentrations decrease within the first sample of Site 824 from a seawater value of 556.43 mM to 540.97 mM (Table 2 and Fig. 11). With increasing depth below this sample, the chloride concentration increases to concentrations similar to that of seawater.

Alkalinity, Sulfate, and Ammonia

Alkalinity, sulfate, and ammonia concentrations did not vary significantly downhole at Site 824, reflecting the low organic matter contents and minimal amount of sulfate reduction occurring at this site (Table 2 and Fig. 12).

Silica

Silica concentrations were nearly constant at 100 μM throughout all of the samples (Table 2 and Fig. 13) at this site. Concentrations are low due to the small amount of biogenic silica in the sediments, as shown by micropaleontological analysis.

Carbonate Content and X-ray Diffraction Data

Samples for X-ray diffraction (XRD) analyses were taken from IW squeeze cakes and physical properties samples. X-ray analysis at Site 824 indicates that the sediments in the top 119.4 mbsf are greater than 34% aragonite (Table 3 and Fig. 14). Aragonite concentrations reach values of 75.8% near the top of the hole and decrease with increasing depth. Below 257.2 mbsf, aragonite is absent. Calcite concentrations increase downhole from 24.2% near the top of Site 824 to 100% at the bottom of the cored interval (Table 3 and Fig. 14). Quartz is absent in all but one sample at Site 824, indicating low sediment input from the continent (Table 3 and Fig. 14). Small amounts of dolomite were present between 95.4 and 238.6 mbsf with concentrations of 0.2%–1.2 % (Table 3 and Fig. 14).

Calcium carbonate values range from 93%–100% and have a high degree of fluctuation in the data (Table 4 and Fig. 15). Using a running average for every five points, distinct trends

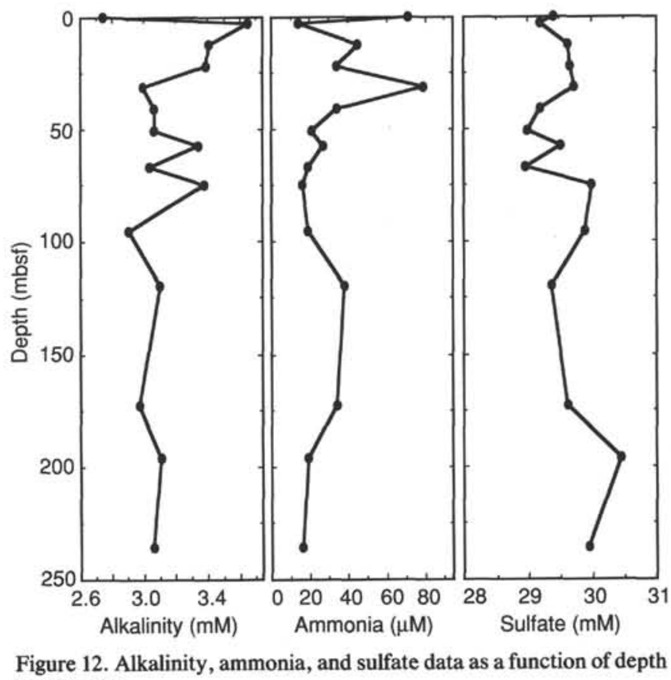

Figure 12. Alkalinity, ammonia, and sulfate data as a function of depth for Site 824.

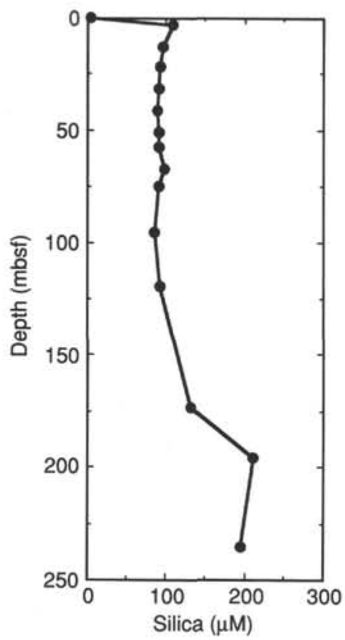

Figure 13. Interstitial-water silica data for Site 824.

of cyclic carbonate variations can be seen (Fig. 15). These variations result from dilution of the carbonate fraction of the sediment by varying amounts of terrigenous inputs. In general there is a trend of increasing carbonate content with increasing depth.

ORGANIC GEOCHEMISTRY

In addition to safety monitoring for hydrocarbons, the main purpose of the shipboard organic geochemistry studies at Site 824 was to assess the amount and origin of the organic matter preserved in the Pleistocene to Miocene carbonate sediments deposited on the western upper slope of the Queensland Plateau.

Samples

Twenty samples were collected from Holes 824A and 824B at 10-m intervals over the depth range from 3 to 257 mbsf. All sediments were analyzed for their composition of light hydrocarbons (C_1–C_3) using headspace analyses. These were analyzed for total nitrogen, sulfur, and carbon, using a NA 1500 Carlo Erba NCS analyzer. Detailed descriptions of methods are outlined in our "Explanatory Notes" chapter (this volume).

Volatile Hydrocarbons

Hydrocarbon gases in sediments were analyzed as part of the safety and pollution-prevention monitoring program, using the headspace technique and the Carle gas chromatograph (for determination of C_1–C_3 concentrations). The results of 21 headspace analyses from Site 824 are presented in Table 5.

The sediments contained low concentrations of methane (between 2 and 12 ppm), which represented no safety and/or pollution hazards. Ethane and propane were not detected.

Organic Carbon Contents

The total organic carbon (TOC) contents recorded in Site 824 are presented in Table 6. The amount of organic carbon was very low in the carbonate-rich sediments, and did not exceed 0.25% TOC. The total nitrogen and sulfur concentrations were below the detection limits of the NCS analyzer.

Table 3. X-ray diffraction data for Site 824.

Core, section, interval (cm)	Depth (mbsf)	Calcite (%)	Aragonite (%)	Quartz (%)	Dolomite (%)
133-824B-					
1H-2, 145–150	2.95	37.7	62.3	0.0	0.0
2H-4, 145–150	10.95	50.5	49.5	0.0	0.0
3H-3, 145–150	18.95	36.3	63.7	0.0	0.0
4H-4, 145–150	29.95	26.1	73.9	0.0	0.0
6H-6, 145–150	51.95	24.2	75.8	0.0	0.0
133-824A-					
1H-5, 140–150	57.40	66.3	33.7	0.0	0.0
2H-5, 140–150	66.90	46.3	53.7	0.0	0.0
3H-4, 140–150	74.90	35.3	64.7	0.0	0.0
5H-5, 140–150	95.40	62.6	36.7	0.0	0.7
8H-2, 140–150	119.40	58.3	41.7	0.0	0.0
14H-5, 140–150	173.10	98.0	0.0	0.8	1.2
17X-2, 140–150	196.90	91.5	8.2	0.0	0.4
21X-4, 140–150	238.60	95.9	3.9	0.0	0.2
133-824C-					
1R-CC, 0–5	257.20	100.0	0.0	0.0	0.0
7R-CC, 0–5	305.40	100.0	0.0	0.0	0.0
133-824A-29X-CC, 0–5	319.50	100.0	0.0	0.0	0.0
133-824C-8R-CC, 0–0	324.80	96.4	3.6	0.0	0.0

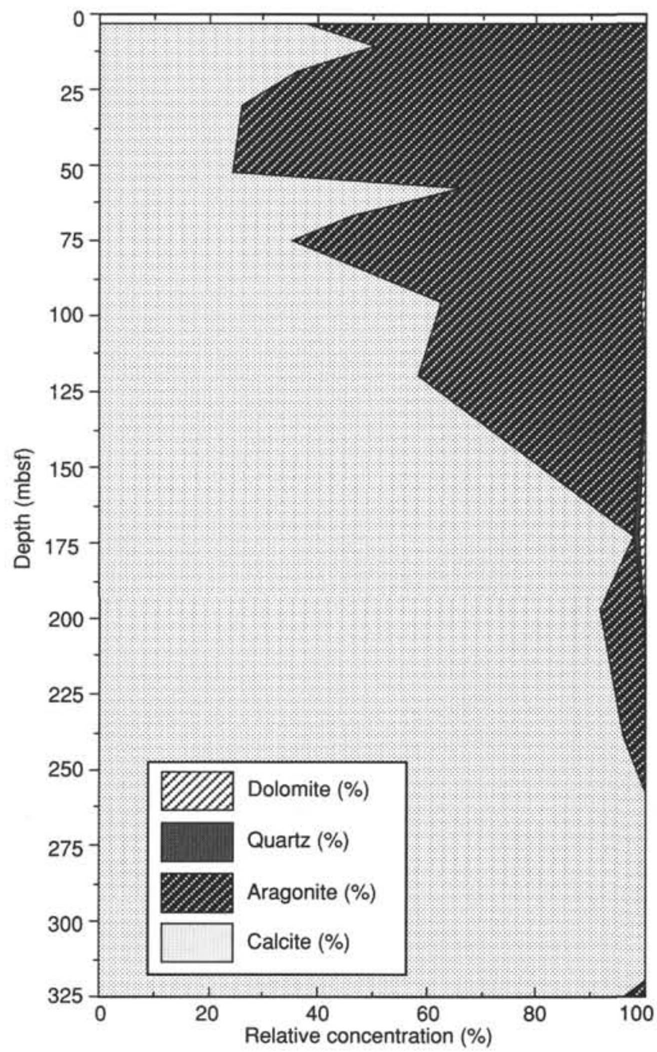

Figure 14. X-ray diffraction data as a function of depth for Site 824.

As a consequence of the low organic contents, we were unable to conduct detailed geochemical characterization of kerogen types using the Rock-Eval pyrolysis method, asoriginally planned. More detailed shore-based studies (elemental analysis and optical investigations on extracted kerogens) will permit characterization of the organic matter preserved in the sediments encountered at Site 824.

PHYSICAL PROPERTIES

Physical properties data from Site 824 appear in Tables 7–9, and are plotted vs. depth in Figures 16 through 18. From the seafloor to ~245 mbsf, two basic units can be identified in terms of index properties of Site 824. Unit A extends from the seafloor to 73 mbsf and consists predominantly of bioclastic nannofossil and foraminifer ooze. Normal compaction trends are observed, i.e., increasing bulk density and corresponding decrease in porosity (Fig. 18C) and water content (Fig. 18D). Bulk-density values increase from 1.6 g/cm^3 near the seafloor to ~1.8 g/cm^3 at 73 mbsf, with an increasing rate of about 0.29 g/cm^3/100 m. Grain densities (Fig. 18B) exhibit a considerable variability, but maintain an average value of 2.74 ±0.05 g/cm^3. Porosity decreases from 66% near the seafloor to about 60% at 73 mbsf, with a decreasing rate of 8.6%/100 m. Water content ranges from ~64% to 54%, with a decreasing rate of 13.6%/100 m for the same interval.

Unit B extends from 73 mbsf to the last sample tested at 244.8 mbsf. The index property data shows less variability than the shallower unit and remains relatively constant with depth. Bulk densities remain ~1.81 ±0.05 g/cm^3. Grain densities remain ~2.71 ±0.05 g/cm^3. In addition, porosity remains at 56 ±2.4 % and water content at 46.5 ±4.1%.

P-wave velocities and vane shear strengths (Figs. 18E and 18F) exhibited large variations. *P*-wave velocity values range between 1.4 and 1.7 km/s. The coarse-grained sediments which have velocity values <1.5 km/s, were unsaturated with the seawater when they were measured in the Hamilton Frame apparatus. Vane-shear-strength data varied mostly below 10 kPa for the upper 175-m interval.

DOWNHOLE MEASUREMENTS

Log Reliability

Hole size and condition are the most important controls on accuracy of logs from Hole 824D, and the caliper is the best indicator of these parameters. Most of the logged interval was greater than 15 in. (38 cm) in diameter, based on both mechanical and sonic calipers (see "Explanatory Notes" chapter, this volume). We had anticipated very large hole size and had decided not to run the lithodensity tool, which requires pad contact against the borehole wall. Most other logs do not require pad contact and therefore are relatively insensitive to changes in borehole size; the gamma-ray and resistivity logs probably will be changed slightly by post-cruise borehole correction.

As is often the case with ODP holes, the initial sonic logs from Hole 824D exhibited some zones in which cycle skipping caused unreliable swings in apparent velocity. Reprocessing (see "Explanatory Notes" chapter, this volume) was successful in removing most but not all unreliable data. Therefore we have created a composite reprocessed velocity log by combining the most reliable portions of three runs: the downgoing log, the repeat section upgoing log, and the main upgoing log (Fig. 19). We consider the merged reprocessed log of Figure 19 to be of generally good quality, but we are suspicious of the quality of two intervals (133–138 mbsf and 288–318 mbsf) that exhibit a fair-to-poor correlation with resistivity.

The spectral gamma-ray tool is the only tool on the seismic stratigraphic combination that can provide useful formation data even through pipe. At Hole 824D through-pipe spectral gamma-ray logs were obtained for the interval 0–61 mbsf, but values for uranium, thorium, and potassium are all near or below the resolving power of the tool. For this through-pipe interval, total gamma-ray signal is above the noise level of the tool; however, pipe-correction of these data has not been undertaken yet. For the open-hole interval, replicate spectral gamma-ray logs show modest agreement for uranium and almost no agreement for both potassium and thorium. The latter two elements are present in such low quantities at Hole 824D that their logs fluctuate about zero, and the total gamma log is almost entirely attributable to uranium (Fig. 20).

Velocity and Resistivity

Velocity and resistivity are moderately correlated throughout most of the logged interval at Hole 824D (Figs. 19 and 20). Because lithologic changes are relatively minor and confined to variations in relative proportions of the geophysically rather similar minerals dolomite and calcite, log responses are controlled almost entirely by porosity.

The increase in velocity with depth appears to follow a simple compaction profile only in the top 280 mbsf. Velocities increase from 1.7 km/s at 60 mbsf to 2.1 km/s at 280 mbsf, not greatly different from the velocities of 1.67 and 2.0 km/s observed at similar depths in pelagic carbonates (Hamilton, 1979); comparable data for near-reef carbonates are rare. Thus, mechanical compaction may be more important than diagenesis in controlling porosities in the top 280 mbsf. Below 280 mbsf, however, velocities are much higher than in pelagic carbonates of comparable depth, suggesting that diagenesis affects porosity much more than does mechanical compaction. A similar dominance of diagenesis was seen at Site 812 (see "Site 812" chapter, this volume). There are several zones in which resistivity and velocity decrease with increasing depth, contrary to the normal compaction profile. This agrees with the drilling experience, where soft intervals were encountered below hard layers, resulting in poor core recovery.

Velocity and resistivity ratios have been taken to remove the effects of water velocity and resistivity and to display differences between the two porosity-sensitive logs, which are usually assumed to move together (Fig. 21). Here, excursions to large positive *A/B* ratios indicate that velocity is high in comparison to resistivity, as should be the case for a highly porous sediment in which grain contacts have been cemented. No such zones are evident at Site 824. Excursions to low *A/B* ratios may be generated if velocity remains constant and resistivity increases, as might happen should the grains of an unconsolidated sediment become more platy at a constant porosity or should a cemented sediment have unconnected pores. Several zones of low *A/B* ratios are evident in Figure 21, corresponding with the highest resistivity intervals. Velocity and resistivity in these intervals are too high to be unconsolidated, and the second possibility, of unconnected pores may be more likely. In particular, unconnected pores of diagenetic origin may be the most likely explanation for the interval from 282 to 326 mbsf, where a conjunction of very high resistivities and only moderately high (but variable) velocities. The log "Thin R" (Fig. 21) can provide a qualitative indicator of frequency of thin beds (see "Site 812" chapter, this volume). This log delineates thin resistive layers by taking a ratio of the shallow high-resolution SFL and the deeper-penetrating but lower-resolution induction log. Oe can see that "Thin R" logs are sensitive to instantaneous changes in resistivity caused by high-contrast thick beds, in addition to

Table 4. Carbonate data for Site 824.

Core, section, interval (cm)	Depth (mbsf)	Sample code	Total carbon (%)	Inorganic carbon (%)	Organic carbon (%)	$CaCO_3$ (%)
133-824B-						
1H-1, 103–106	1.03	PP		11.55		96.2
1H-2, 100–103	2.50	PP		11.38		94.8
1H-2, 145–150	2.95	IW	11.56	11.55	0.01	96.2
1H-3, 100–103	4.00	PP		11.45		95.4
2H-1, 100–103	6.00	PP		11.64		97.0
2H-2, 104–107	7.54	PP		11.63		96.9
2H-3, 91–94	8.91	PP		11.70		97.5
2H-4, 111–114	10.61	PP		11.64		97.0
2H-5, 99–100	11.99	PP		11.59		96.5
2H-5, 145–150	12.45	IW	11.75	11.73	0.02	97.7
2H-6, 100–103	13.50	PP		11.68		97.3
3H-1, 97–100	15.47	PP		11.49		95.7
3H-2, 97–100	16.97	PP		11.69		97.4
3H-3, 97–100	18.47	PP		11.42		95.1
3H-4, 97–100	19.97	PP		11.36		94.6
3H-5, 97–100	21.47	PP		11.49		95.7
3H-5, 145–150	21.95	IW	11.68	11.67	0.01	97.2
3H-6, 97–100	22.97	PP		11.58		96.5
4H-1, 94–96	24.94	PP		11.62		96.8
4H-2, 94–96	26.44	PP		11.65		97.0
4H-3, 94–96	27.94	PP		11.65		97.0
4H-4, 94–96	29.44	PP		11.63		96.9
4H-5, 94–96	30.94	PP		11.41		95.0
4H-5, 145–150	31.45	IW	11.89	11.82	0.07	98.5
4H-6, 94–96	32.44	PP		11.48		95.6
5H-1, 97–100	34.47	PP		11.52		96.0
5H-2, 97–100	35.97	PP		11.64		97.0
5H-3, 97–100	37.47	PP		11.67		97.2
5H-4, 97–100	38.97	PP		11.62		96.8
5H-5, 97–100	40.47	PP		11.73		97.7
5H-5, 145–150	40.95	IW	11.81	11.77	0.04	98.0
5H-6, 97–100	41.97	PP		11.65		97.0
6H-1, 100–103	44.00	PP		11.67		97.2
6H-2, 100–103	45.50	PP		11.61		96.7
6H-3, 100–103	47.00	PP		11.67		97.2
6H-4, 100–103	48.50	PP		11.67		97.2
6H-5, 100–103	50.00	PP		11.69		97.4
6H-5, 145–150	50.45	IW	11.75	11.74	0.01	97.8
824A-1H-1, 100–103	51.00	PP		11.59		96.5
824B-6H-6, 100–103	51.50	PP		11.68		97.3
824A-1H-2, 100–103	52.50	PP		11.63		96.9
1H-3, 100–103	54.00	PP		11.55		96.2
1H-4, 100–103	55.50	PP		11.79		98.2
1H-5, 100–103	57.00	PP		11.68		97.3
1H-5, 140–150	57.40	IW	11.82	11.69	0.13	97.4
1H-6, 100–103	58.50	PP		11.70		97.5
2H-1, 101–103	60.51	PP		11.75		97.9
2H-2, 101–103	62.01	PP		11.72		97.6
2H-3, 101–103	63.51	PP		11.81		98.4
2H-4, 101–103	65.01	PP		11.78		98.1
2H-5, 101–103	66.51	PP		11.73		97.7
2H-5, 140–150	66.90	IW	11.78	11.59	0.19	96.5
2H-6, 101–103	68.01	PP		11.69		97.4
3H-1, 100–103	70.00	PP		11.64		97.0
3H-2, 100–103	71.50	PP		11.40		95.0
3H-3, 100–103	73.00	PP		11.80		98.3
3H-4, 100–103	74.50	PP		11.94		99.5
3H-4, 140–150	74.90	IW	11.79	11.67	0.12	97.2
3H-5, 100–103	76.00	PP		11.77		98.0
3H-6, 100–103	77.50	PP		11.64		97.0
5H-1, 100–103	89.00	PP		11.89		99.0
5H-2, 100–103	90.50	PP		11.68		97.3
5H-3, 100–103	92.00	PP		11.81		98.4
5H-4, 100–103	93.50	PP		11.81		98.4
5H-5, 100–103	95.00	PP		11.76		98.0
5H-5, 140–150	95.40	IW	11.94	11.82	0.12	98.5
5H-6, 100–103	96.50	PP		11.41		95.0
6H-1, 101–103	98.51	PP		11.70		97.5
6H-2, 101–103	100.01	PP		11.72		97.6
6H-3, 101–103	101.51	PP		11.70		97.5
6H-4, 101–103	103.01	PP	11.78	11.60	0.18	96.6
6H-5, 101–103	104.51	PP		11.66		97.1
6H-6, 101–103	106.01	PP		11.69		97.4
7H-1, 100–103	108.00	PP		11.53		96.0
7H-2, 100–103	109.50	PP		11.64		97.0

Table 4 (continued).

Core, section, interval (cm)	Depth (mbsf)	Sample code	Total carbon (%)	Inorganic carbon (%)	Organic carbon (%)	$CaCO_3$ (%)
7H-3, 100–103	111.00	PP		11.77		98.0
7H-4, 100–103	112.50	PP	11.68	11.67	0.01	97.2
8H-1, 100–103	117.50	PP		11.82		98.5
8H-2, 100–103	119.00	PP		11.68		97.3
8H-2, 140–150	119.40	IW	11.84	11.69	0.15	97.4
8H-3, 100–103	120.50	PP		11.69		97.4
8H-4, 100–103	122.00	PP		11.71		97.5
8H-5, 100–103	123.50	PP		11.73		97.7
8H-6, 100–103	125.00	PP		11.76		98.0
9H-1, 100–103	127.00	PP		11.59		96.5
9H-2, 100–103	128.50	PP		11.66		97.1
9H-3, 100–103	130.00	PP	11.90	11.68	0.22	97.3
9H-4, 100–103	131.50	PP		11.59		96.5
9H-5, 100–103	133.00	PP		11.52		96.0
9H-6, 100–103	134.50	PP		11.68		97.3
14H-1, 100–103	166.70	PP		11.96		99.6
14H-2, 100–103	168.20	PP		11.78		98.1
14H-3, 100–103	169.70	PP		11.66		97.1
14H-4, 100–103	171.20	PP		11.68		97.3
14H-5, 100–103	172.70	PP		11.75		97.9
14H-5, 140–150	173.10	IW	11.67	11.59	0.08	96.5
14H-6, 100–103	174.20	PP		11.64		97.0
15H-1, 102–105	176.22	PP		11.82		98.5
15H-2, 100–103	177.70	PP		11.78		98.1
15H-3, 115–117	179.35	PP		11.91		99.2
15H-4, 100–103	180.70	PP	12.09	11.93	0.16	99.4
15H-5, 100–103	182.20	PP		11.88		99.0
15H-6, 100–103	183.70	PP		11.92		99.3
17X-1, 100–103	195.00	PP		11.82		98.5
17X-2, 100–103	196.50	PP		11.89		99.0
17X-2, 145–150	196.95	IW	11.96	11.84	0.12	98.6
17X-3, 100–103	198.00	PP		11.75		97.9
17X-4, 30–33	198.80	PP		11.81		98.4
19X-1, 100–103	214.30	PP		11.66		97.1
19X-2, 100–103	215.80	PP		11.89		99.0
19X-3, 100–103	217.30	PP		11.81		98.4
19X-4, 100–103	218.80	PP	11.65	11.64	0.01	97.0
19X-5, 100–103	220.30	PP		11.63		96.9
19X-6, 100–103	221.80	PP		11.64		97.0
21X-1, 100–103	233.70	PP		11.77		98.0
21X-2, 100–103	235.20	PP		11.81		98.4
21X-2, 140–150	235.60	IW	11.86	11.74	0.12	97.8
21X-3, 100–103	236.70	PP		11.72		97.6
22X-1, 100–103	243.30	PP		11.88		99.0
22X-2, 100–103	244.80	PP	11.99	11.83	0.16	98.5
29X-CC, 0–1	309.90	IW	12.21	12.00	0.21	100.0

IW = interstitial water sample; PP = physical properties sample.

thin beds that remain outside the resolving power of the measurements.

The reprocessed sonic log has been converted to an integrated traveltime log (Fig. 22), to facilitate depth-to-time conversion for comparison of Site 824 data with seismic sequences. For the unlogged interval between the seafloor and 60.5 mbsf, we used a simple linear interpolation between water velocity at the seafloor and the first log value at 60.5 mbsf. We subjectively estimate an error of <6 ms associated with uncertainties of velocities in the top 60.5 mbsf.

Log-based Units

Based on log responses, Site 824 is composed of at least five units: log Unit 1 (above 95 mbsf), log Unit 2 (between 95 and 282 mbsf), log Unit 3 (between 282 and 326 mbsf), log Unit 4 (between 326 and 405 mbsf), and log Unit 5 (below 405 mbsf).

Most of log Unit 1 was logged only through pipe, and interpretation of this through-pipe data awaits post-cruise pipe correction. Open-hole logs for the interval below 61 mbsf show that log Unit 1 is characterized by high uranium content

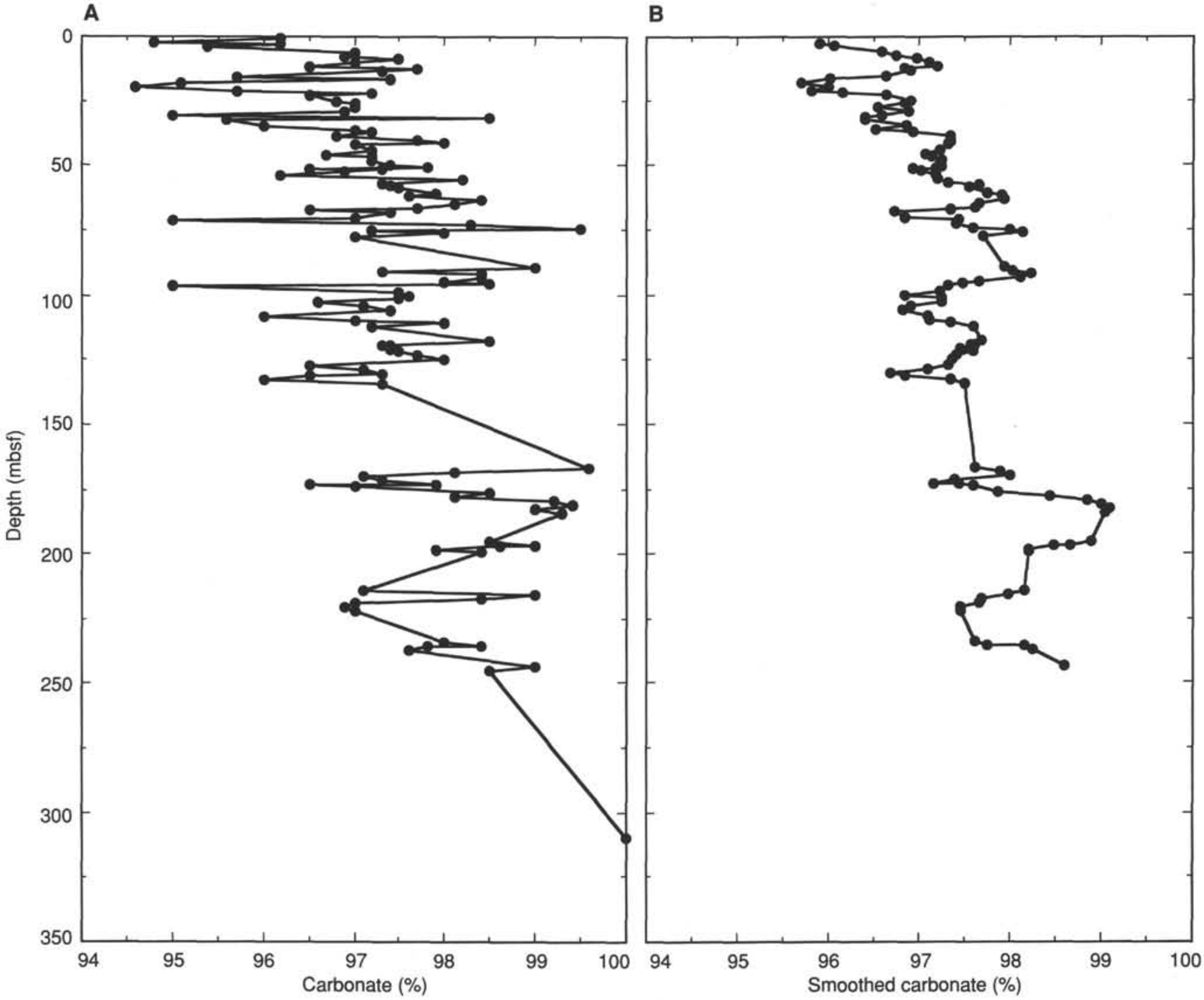

Figure 15. **A.** Carbonate values for Site 824. **B.** Smoothed carbonate values for Site 824.

(Fig. 20), in comparison to log units below 95 mbsf. Uranium content is much higher than is typical of pelagic carbonate. However, in other respects the log responses in this unit are typical of pelagic carbonates at similar depths.

Log responses of log Unit 2 (95–282 mbsf) are surprisingly homogeneous in view of the lithostratigraphic heterogeneity identified in core descriptions for these unlithified carbonate oozes (see "Lithostratigraphy" section, this chapter). However, three more lithified beds are obvious from the resistivity and velocity logs (Fig. 20): 132–137, 163–167, and 251–260 mbsf. These beds may correlate with at least two, and possibly three, lithologic unit boundaries: the Unit II/III boundary at 135.5 mbsf, the Unit III/IV boundary at 166 mbsf, and the Unit IV/V boundary at 242.3 mbsf (see "Lithostratigraphy" section, this chapter). These three beds are probably rich in bioclasts, which are more lithified than the ooze. Further, two uranium spikes, at 200 mbsf and 263 mbsf, may indicate influxes of unlithified but geochemically distinctive reef-derived material.

Log Unit 3 (282–326 mbsf) is most distinctive in the resistivity log, where it is characterized by very high resistivities in general and an overall pattern of gradually decreasing resistivity uphole. These features are less developed on the velocity log. The high-frequency character of this portion of the velocity log might be real, with the higher resolution of velocity capable of picking up thin beds that are beyond the resolution of the resistivity log. However, we suspect that this spikiness is at least partially caused by artifacts in this noisy portion of the log, because replicability here is only fair (Fig. 19); no FMS logs were obtained; thus, we cannot resolve this question. The decrease to Unit 4 velocities in the interval from 308 to 317 mbsf may be real on the basis of its replicability (Fig. 19); if so, the high resistivities for this interval suggest that the pores lack connectivity.

This unit is much higher in resistivity and velocity than overlying and underlying units, implying much lower porosity. As even the overlying and underlying units are lower than typical pelagic carbonates in porosity, log Unit 3 porosities imply substantial diagenetic cementation. This diagenetic cementation must be quite variable with depth, as seen by the highly variable velocities and resistivities (Fig. 20). Very thin beds with near-zero porosity are seen in the resistivity log at 298 and 319 mbsf.

Log responses in log Unit 3 are most consistent with a control of porosity by shallow-water or subaerial diagenesis. Near-zero porosities of some horizons imply thorough cemen-

Table 5. Volatile hydrocarbon data from headspace analyses at Site 824.

Core, section, interval (cm)	Depth (mbsf)	Sample	Volume (mL)	Gas chromato.	C_1 (ppm)	C_{2+} (ppm)
133-824B-						
1H-2, 149–150	2.99	HS	5	CAR132	2	0
2H-5, 149–150	12.49	HS	5	CAR132	2	0
3H-5, 149–150	21.99	HS	5	CAR132	2	0
4H-5, 149–150	31.49	HS	5	CAR132	2	0
5H-5, 149–150	40.99	HS	5	CAR132	2	0
6H-5, 149–150	50.49	HS	5	CAR132	2	0
133-824A-						
1H-5, 140–141	57.4	HS	5	CAR132	12	0
2H-5, 149–150	66.99	HS	5	CAR132	3	0
3H-4, 140–141	74.9	HS	5	CAR132	3	0
4H-5, 0–2	84.5	HS	5	CAR132	2	0
5H-5, 149–150	95.49	HS	5	CAR132	3	0
6H-6, 0–2	105	HS	5	CAR132	3	0
7H-6, 0–2	114.5	HS	5	CAR132	3	0
8H-5, 0–2	122.5	HS	5	CAR132	2	0
14H-5, 149–150	173.19	HS	6	CAR132	3	0
15H-5, 149–150	182.69	HS	5	CAR132	2	0
17X-2, 149–150	196.99	HS	5	CAR132	4	0
19X-6, 149–150	222.29	HS	5	CAR132	2	0
21X-2, 149–150	235.69	HS	5	CAR132	3	0
824C-2R-CC, 0–1	257.2	HS	5	CAR132	3	0

HS = headspace sample.

Table 6. Concentrations of total organic carbon, inorganic carbon, and total carbon in interstitial water and physical properties samples from Site 824.

Core, section, interval (cm)	Depth (mbsf)	Sample	Total organic carbon (%)	Total inorganic carbon (%)	Total carbon (%)
133-824B-					
1H-2, 145–150	2.95	IW	0.01	11.55	11.56
2H-5, 145–150	12.45	IW	0.02	11.73	11.75
3H-5, 145–150	21.95	IW	0.01	11.67	11.68
4H-5, 145–150	31.45	IW	0.07	11.82	11.89
5H-5, 145–150	40.95	IW	0.04	11.77	11.81
6H-5, 145–150	50.45	IW	0.01	11.74	11.75
133-824A-					
1H-5, 140–150	57.4	IW	0.13	11.69	11.82
2H-5, 140–150	66.9	IW	0.19	11.59	11.78
3H-4, 140–150	74.9	IW	0.12	11.67	11.79
5H-5, 140–150	95.4	IW	0.12	11.82	11.94
6H-4, 101–103	103.01	PP	0.18	11.6	11.78
7H-4, 100–103	112.5	PP	0.01	11.67	11.68
8H-2, 140–150	119.4	IW	0.15	11.69	11.84
9H-3, 100–103	130	PP	0.22	11.68	11.9
14H-5, 140–150	173.1	IW	0.08	11.59	11.67
15H-4, 100–103	180.7	PP	0.16	11.93	12.09
17X-2, 145–150	196.95	IW	0.12	11.84	11.96
19X-4, 100–103	218.8	PP	0.01	11.64	11.65
21X-2, 140–150	235.6	IW	0.12	11.74	11.86
22X-2, 100–103	244.8	PP	0.16	11.83	11.99
29X-CC, 0–1	309.9	IW	0.21	12	12.21

IW = interstitial water sample; PP = physical properties sample.

tation; yet horizons only a meter deeper or shallower have substantial porosity, possibly caused by dissolution. This diagenetic pervasiveness and heterogeneity contrasts markedly with overlying log Unit 2, which has little log-based evidence of diagenesis. Thus, deposition and diagenesis of log Unit 3 may have been followed by substantial subsidence and then deposition of log Unit 2. The cause of the broad trend of upwardly decreasing diagenesis within log Unit 3 and into log Unit 2 is thought to be deepening upward (see "Lithostratigraphy" section, this chapter).

Log Unit 4 (326–405 mbsf) apparently is a uniform chalk, based on log responses. Exceptions to this general homogeneous character are several very thin beds, which give rise to small resistivity spikes, and a significant downhole increase in uranium at 379 mbsf. Velocities in this unit are higher than can be accounted for by mechanical compaction, and some cementation is likely. The homogeneity of porosities suggests that the cementation may have occurred in greater water depths than that characterizing log Unit 3.

Log Unit 5 is basement. Because of a very high rate of caving in Hole 824D, only the top 2–3 m of basement were logged. As is evident in the resistivity log (Fig. 20), basement porosities are distinctively low. Though this single resistivity spike offers minimal insight into the characteristics of basement at Site 824, it does confirm that the logs have captured the entire sedimentary sequence at this site.

SEISMIC STRATIGRAPHY

The seismic stratigraphic data for Site 824, obtained by comparison of the seismic analysis with the sedimentological data, is outlined below. The time-depth velocity plot (shown in Fig. 6, "Site Geophysics" chapter, this volume) was calculated during the cruise to compare seismic data with drilling results and to predict lithologies in advance of drilling. An interpretation of the seismic stratigraphy at Site 824 is shown in Figure 23 and a comparison with the lithostratigraphic logs in Figure 24. Four seismic stratigraphic sequences were identified and are shown in Figures 23 and 24.

Sequence 1 occurs only in the vicinity of the drill site, having been eroded both up- and downslope. It is ~70 ms (TWT) thick at the drill site and occurs largely within the source pulse, making its characterization difficult. However, high-amplitude mounding between the base of the source pulse and the base of the sequence is indicated.

Sequence 2 is 130 ms (TWT) thick at the drill site, but thins eastward and westward due to truncation by the seafloor. It is composed of high-amplitude mounded reflectors except in shallow water to the east, where it has both high- and low-amplitude continuous reflector characteristics.

Sequence 3 is a uniformly thick sequence, being 110 ms thick except immediately east of the drill site, where it swells to 150 ms (TWT). To the west of the drill site and in its upper two thirds, sequence 3 is composed of high-amplitude continuous reflectors that are seen eastward to onlap the top of sequence 4. Throughout, facies differences within the sequence are indicated by zones of transparency or low amplitude. The reflector at the base of sequence 3 truncates the sequence below.

Sequence 4 is 150 ms thick at the drill site, thinning westward to the edge of the basement block and east toward the reef. At its base, a distinctive mound is intersected by the drill site. Throughout, the sequence is composed of high-amplitude reflectors forming small intersecting mounds.

Sequence 5 is the basement of indeterminate age and thickness. Its upper surface forms a very strong planated reflector, which is downfaulted to the west. Sequence 6 appears to underlie the reef to the east.

The comparison of the seismic data with the pre-drilling program and the post-drilling lithologic units are shown in Figure 24. The boundary between seismic sequences 1 and 2 occurs at or close to the contact of lithologic Subunits IC and ID, which is the boundary between ooze and packstone. Similarly, the boundary between seismic sequences 2 and 3 occurs in a position approximately equivalent to the contact between lithologic Units III and IV, i.e., between bioclastic packstones and rudstones overlying nannofossil oozes. The boundary between seismic sequence 3 and 4 does not correlate with a lithologic unit boundary but does appear to correlate with a facies change from allodapic limestones above to shallow-water reef rubble below. The mounded reflectors within sequence 4 correlate with the lithologies described within lithologic Unit VI as bryozoans, mollusks, and coralline algae.

SUMMARY AND CONCLUSIONS

Overview

Site 824 was located on the western slope of the Queensland Plateau to study sedimentation processes along the eastern margin of the Queensland Trough and to identify the earliest Paleogene sediments which transgressed across the basement complex. Drilling yielded a latest Oligocene–earliest Miocene to Pleistocene record strongly influenced by redeposition from the nearby Holmes Reef platform. Based on initial shipboard results, a preliminary sedimentation history consistent with data gathered at other Leg 133 drill sites on the Queensland Plateau evolved.

Sedimentation History

Basement lithologies recovered at Site 824 comprise phyllites and basic metavolcanics capped by a deeply weathered regolith. A marine transgression across this continental basement apparently began in the latest Oligocene–earliest Miocene with the deposition of a bryozoan rudstone containing abundant fragments of corallinacean algae, mollusks, larger foraminifers and tiny (ahermatypic?) corals. This bio-assemblage may represent a deep-water biostrome or more probably a shallow-water temperate to subtropical deposit. A subsequent dramatic change to a tropical reefal bio-assemblage in the overlying middle Miocene sediments indicates that the transition from temperate–subtropical to tropical conditions must have been relatively rapid, too rapid to be explained exclusively by the northward movement of the Australian plate. The rapid transition probably reflects major changes in the regional paleocirculation pattern with an enhanced southward flow of warm equatorial surface water along the northeast Australian margin.

Poor recovery and poor fossil preservation in the sedimentary sequence limit the time resolution of stratigraphic events, but an initial record of changing environmental conditions and erosional processes on the neighboring Holmes Reef platform can be gleaned from the sediments. During the transition from the middle to late Miocene, the dominant sediment type changed from bioclastic rudstone and packstone to a nannofossil ooze or chalk with varying amounts of redeposited shallow-water components. An increased pelagic component in the sediments deposited across the middle to late Miocene transition has also been recognized at nearby Sites 811 and 825, which are located east of Holmes Reef, and may likewise represent decreased production on the carbonate banks during the late Miocene.

The directly overlying lower Pliocene sediments are again bioclastic packstone and rudstone that are interpreted to be proximal debris deposits from the nearby tropical reef. This reappearance of significant amounts of reefal debris at Site 824 may represent a reactivation of the shallow-water environment in association with a major decline in sea level at ~3.9 Ma.

In summary, even considering the poor recovery and poor fossil preservation at Site 824, the sequence does contain a record in the redeposited sediments of paleoenvironmental and sea-level changes occurring in shallower waters on the Holmes Reef platform. This record can be correlated, in turn, to more complete stratigraphic sequences at nearby Sites 811 and 825 and the other more distant drill sites on the Queensland Plateau. Shore-based studies promise to provide more detailed information to extract the climatic and sea-level information stored in this interesting sequence.

REFERENCES

Burns, R. E., Andrews, J. E., et al., 1973. *Init. Repts. DSDP,* 21: Washington (U.S. Govt. Printing Office).

Feary, D. A., Pigram, C. J., Davies, P. J., Symonds, P. A., Droxler, A. W., and Peerdeman, F., 1990. Ocean Drilling Program–Leg 133 Safety package. *Bur. Miner. Res. Aust. Rec.,* 1990/6.

Hamilton, E. L., 1979. Sound velocity gradients in marine sediments. *J. Acoust. Soc. Am.,* 65:909–922.

Mutter, J. C., and Karner, G. D., 1980. The continental margin off northeast Australia. *In* Henderson, R. A., and Stephenson, P. J. (Eds), *The Geology and Geophysics of Northeast Australia.* Geol. Soc. Aust. Queensland Div., 47–69.

Schlager, W., and James, N. P., 1978. Low-magnesian calcite limestones forming at the deep-sea floor, Tongue of the Ocean, Bahamas. *Sedimentology,* 15:675–702.

Symonds, P. A., and Davies, P. J., 1988. Structure, stratigraphy, evolution and regional framework of the Townsville Trough and Marion Plateau region–research cruise proposal, project 9131.11. *Bur. Miner. Res. Aust. Rec.,* 1988/48.

van Morkhoven, F.P.C.M., Berggren, W. A., and Edwards, A. S., et al., 1986. Cenozoic cosmopolitan deep-water benthic foraminifera. *Bull. Cent. Rech. Explor.-Prod. Elf-Aquitaine,* Mem. 11.

133A-117

NOTE: All core description forms ("barrel sheets") and core photographs have been printed on coated paper and bound separately as Part 2 of this volume, beginning on page 813.

Table 7. Index properties data for Site 824.

Core, section, interval (cm)	Depth (mbsf)	Bulk density (g/cm^3)	Grain density (g/cm^3)	Porosity (%)	Water content (%)	Void ratio
133-824B-						
1H-1, 103–106	1.03	1.73	2.70	66.0	64.4	1.94
1H-2, 100–103	2.50	1.68	2.73	63.7	63.2	1.75
1H-3, 100–103	4.00	1.60	2.68	67.0	75.2	2.03
2H-1, 100–103	6.00	1.73	2.75	62.3	58.6	1.65
2H-2, 104–107	7.54	1.69	2.77	63.6	63.0	1.75
2H-3, 91–94	8.91	1.70	2.78	63.5	61.8	1.74
2H-4, 111–114	10.61	1.78	2.68	58.8	51.2	1.43
2H-5, 97–100	11.97	1.63	2.75	55.8	72.4	2.01
2H-6, 100–103	13.50	1.76	2.75	60.1	53.8	1.51
3H-1, 100–103	15.50	1.65	2.71	66.5	70.1	1.98
3H-2, 97–100	16.97	1.80	2.89	58.0	49.4	1.38
3H-3, 97–100	18.47	1.67	2.71	63.7	64.0	1.75
3H-4, 97–100	19.97	1.68	2.76	65.1	66.1	1.87
3H-5, 97–100	21.47	1.83	2.72	56.5	46.2	1.30
3H-6, 97–100	22.97	1.80	2.68	57.9	49.0	1.37
4H-1, 97–100	24.97	1.78	2.72	61.9	55.4	1.63
4H-2, 97–100	26.47	1.78	2.76	60.4	53.2	1.53
4H-3, 97–100	27.97	1.85	2.71	56.8	56.9	1.32
4H-4, 97–100	29.47	1.62	2.68	61.5	63.8	1.60
4H-5, 97–100	30.97	1.61	2.76	68.3	76.6	2.16
4H-6, 97–100	32.47	1.74	2.84	63.2	59.5	1.72
5H-1, 97–100	34.47	1.77	2.77	62.8	57.3	1.69
5H-2, 97–100	35.97	1.70	2.68	65.1	64.2	1.87
5H-3, 97–100	37.47	1.69	2.78	64.3	64.1	1.80
5H-4, 97–100	38.97	1.74	2.82	64.0	60.6	1.78
5H-5, 97–100	40.47	1.91	2.73	53.4	40.3	1.15
5H-6, 97–100	41.97	1.82	2.90	57.2	47.3	1.33
6H-1, 100–103	44.00	1.67	2.76	65.8	67.9	1.93
6H-2, 100–103	45.50	1.81	2.78	58.0	48.6	1.38
6H-3, 100–103	47.00	1.78	2.73	60.1	52.8	1.51
6H-4, 100–103	48.50	1.78	2.67	63.7	58.0	1.75
6H-5, 100–103	50.00	1.70	2.76	61.6	58.8	1.61
6H-6, 100–103	51.50	1.80	2.69	59.2	50.7	1.45
133-824A-						
1H-1, 100–103	51.00	1.80	2.79	65.0	58.5	1.86
1H-2, 100–103	52.50	1.77	2.68	59.2	52.2	1.45
1H-3, 100–103	54.00	1.70	2.81	63.9	62.4	1.77
1H-4, 100–103	55.50	1.81	2.72	55.5	45.6	1.25
1H-5, 100–103	57.00	1.74	2.74	61.1	56.0	1.57
1H-6, 100–103	58.50	1.77	2.89	62.8	57.1	1.69
2H-1, 101–103	60.51	1.68	2.73	64.4	64.6	1.81
2H-2, 101–103	62.01	1.75	2.78	62.2	57.0	1.65
2H-3, 101–103	63.51	1.77	2.80	62.5	56.6	1.67
2H-4, 101–103	65.01	1.78	2.77	59.3	52.0	1.46
2H-5, 101–103	66.51	1.76	2.70	58.7	52.0	1.42
2H-6, 101–103	68.01	1.77	2.76	60.5	54.0	1.53
3H-1, 100–103	70.00	1.74	2.79	62.4	57.8	1.66
3H-2, 100–103	71.50	1.76	2.73	59.0	52.2	1.44
3H-3, 100–103	73.00	1.92	2.67	49.4	35.7	0.98
3H-4, 100–103	74.50	1.83	2.74	56.5	46.3	1.30
3H-5, 100–103	76.00	1.85	2.78	60.6	50.5	1.54
3H-6, 100–103	77.50	1.78	2.75	61.2	54.4	1.58
5H-1, 100–103	89.00	1.81	2.69	56.1	46.6	1.28
5H-2, 100–103	90.50	1.85	2.69	56.4	45.4	1.29
5H-3, 100–103	92.00	1.88	2.77	54.2	41.7	1.18
5H-4, 100–103	93.50	1.94	2.76	51.1	37.0	1.05
5H-5, 100–103	95.00	1.79	2.69	55.9	46.8	1.27
5H-6, 100–103	96.50	1.81	2.69	56.3	46.8	1.29
6H-1, 100–103	98.50	1.77	2.74	59.0	51.7	1.44
6H-2, 100–103	100.00	1.82	2.73	56.5	46.8	1.30
6H-3, 100–103	101.50	1.79	2.71	55.4	46.5	1.24
6H-4, 100–103	103.00	1.79	2.69	61.0	53.8	1.57
6H-5, 100–103	104.50	1.79	2.72	56.7	48.0	1.31
6H-6, 100–103	106.00	1.81	2.72	56.1	46.5	1.28
7H-1, 100–103	108.00	1.77	2.65	56.9	49.2	1.32
7H-2, 100–103	109.50	1.79	2.72	57.3	48.7	1.34
7H-3, 100–103	111.00	1.76	2.77	59.3	52.6	1.46
7H-4, 100–103	112.50	1.81	2.69	57.5	48.1	1.35
8H-1, 100–103	117.50	1.89	2.67	56.2	43.9	1.29
8H-2, 100–103	119.00	1.76	2.73	56.6	49.1	1.31
8H-3, 100–103	120.50	1.72	2.73	57.1	51.6	1.33
8H-4, 100–103	122.00	1.80	2.71	55.5	46.2	1.25
8H-5, 100–103	123.50	1.81	2.71	56.9	47.6	1.32
8H-6, 100–103	125.00	1.81	2.70	56.4	46.7	1.30
9H-1, 100–103	127.00	1.80	2.73	57.2	48.3	1.33
9H-2, 100–103	128.50	1.77	2.70	57.7	50.2	1.36
9H-3, 100–103	130.00	1.84	2.69	53.3	42.1	1.14
133-824A-						
9H-4, 100–103	131.50	1.73	2.71	57.0	51.1	1.33
9H-5, 100–103	133.00	1.85	2.73	54.2	42.7	1.18
9H-6, 100–103	134.50	1.87	2.69	58.9	47.8	1.44
14H-2, 100–103	168.20	1.81	2.67	55.9	46.2	1.27
14H-3, 100–103	169.70	1.78	2.65	55.6	46.9	1.25
14H-4, 100–103	171.20	1.80	2.68	56.8	47.7	1.32
14H-5, 100–103	172.70	1.84	2.69	53.8	42.9	1.17
14H-6, 101–104	174.21	1.80	2.67	56.7	47.7	1.31
15H-1, 102–105	176.22	1.88	2.68	53.8	41.5	1.17
15H-2, 100–103	177.70	1.82	2.67	54.5	44.4	1.20
15H-3, 115–118	179.35	1.85	2.72	53.8	42.3	1.16
15H-4, 100–103	180.70	1.88	2.67	52.5	40.1	1.11
15H-5, 100–103	182.20	1.77	2.66	56.3	48.2	1.29
15H-6, 100–103	183.70	1.97	2.74	47.9	33.2	0.92
17X-1, 100–103	195.00	1.81	2.75	57.7	48.6	1.36
17X-2, 100–103	196.50	1.82	2.86	55.5	45.5	1.25
17X-3, 100–103	198.00	1.76	2.67	57.1	49.7	1.33
17X-4, 30–33	198.80	1.77	2.70	57.6	50.1	1.36
19X-1, 100–103	214.30	1.80	2.84	56.9	48.0	1.32
19X-2, 100–103	215.80	1.84	2.62	54.2	43.2	1.18
19X-3, 100–103	217.30	1.74	2.68	58.1	52.2	1.39
19X-4, 100–103	218.80	1.80	2.68	56.4	47.3	1.30
19X-5, 100–103	220.30	1.80	2.72	57.2	48.4	1.34
19X-6, 100–103	221.80	1.81	2.70	56.8	47.3	1.32
21X-1, 100–103	233.70	1.77	2.63	55.7	47.7	1.26
21X-2, 100–103	235.20	1.84	2.66	53.1	41.9	1.13
21X-3, 100–103	236.70	1.82	2.73	55.7	45.7	1.26
22X-1, 100–103	243.30	1.79	2.87	51.8	42.2	1.08
22X-2, 100–103	244.80	1.84	2.66	53.6	42.5	1.16

Table 8. Compressional-wave velocity data at Site 824.

Core, section, interval (cm)	Depth (mbsf)	Distance (mm)	Traveltime (μs)	Velocity (m/s)
133-824B-				
1H-1, 103–106	1.03	27.67	20.07	1569
1H-2, 100–103	2.50	27.97	20.38	1559
1H-3, 100–103	4.00	25.50	18.86	1551
2H-1, 100–103	6.00	27.37	19.98	1560
2H-2, 104–107	7.54	26.84	19.49	1574
2H-3, 91–94	8.91	27.10	19.46	1593
2H-4, 111–114	10.61	22.41	16.40	1605
2H-5, 97–100	11.97	23.34	17.27	1572
2H-6, 100–103	13.50	27.28	19.25	1626
3H-1, 100–103	15.50	27.48	19.55	1608
3H-2, 97–100	16.97	27.80	19.80	1603
3H-3, 97–100	18.47	29.81	21.30	1582
3H-4, 97–100	19.97	27.92	19.86	1605
3H-5, 97–100	21.47	30.32	21.33	1608
3H-6, 97–100	22.97	29.24	20.58	1615
4H-2, 97–100	26.47	28.98	20.53	1604
4H-3, 97–100	27.97	29.20	20.47	1623
4H-4, 97–100	29.47	30.37	21.76	1573
4H-5, 97–100	30.97	30.64	22.47	1528
5H-5, 97–100	40.47	29.77	22.53	1477
6H-2, 97–100	45.47	30.11	21.43	1587
6H-3, 97–100	46.97	29.37	22.51	1458
6H-4, 97–100	48.47	26.58	18.28	1684
6H-5, 97–100	49.97	29.59	20.85	1610
133-824A-				
2H-1, 100–103	60.50	29.63	21.39	1564
2H-2, 100–103	62.00	28.73	20.53	1590
2H-4, 100–103	65.00	29.80	21.45	1568
2H-5, 100–103	66.50	29.30	20.80	1598
2H-6, 100–103	68.00	29.68	20.57	1642
3H-5, 100–103	76.00	30.16	21.38	1595
5H-2, 100–103	90.50	30.11	20.99	1627
5H-3, 100–103	92.00	28.76	21.75	1485
6H-1, 100–103	98.50	29.11	20.15	1648
6H-2, 100–103	100.00	30.37	23.37	1445
6H-3, 100–103	101.50	26.92	18.98	1630
6H-4, 100–103	103.00	29.30	21.92	1501
6H-5, 100–103	104.50	29.11	22.88	1416
6H-6, 100–103	106.00	28.02	19.41	1656
7H-2, 100–103	109.50	28.21	21.17	1503
7H-3, 100–103	111.00	27.40	21.57	1424
7H-4, 100–103	112.50	25.75	19.96	1463
8H-1, 100–103	117.50	28.15	19.13	1693
8H-3, 100–103	120.50	28.23	19.82	1628
8H-5, 100–103	123.50	26.80	18.75	1647
8H-6, 100–103	125.00	25.75	17.79	1683
9H-4, 100–103	131.50	26.76	19.18	1600
9H-6, 100–103	134.50	26.85	20.58	1475
14H-2, 100–103	168.20	29.15	20.55	1612
14H-3, 100–103	169.70	29.41	20.96	1590
14H-4, 100–103	171.20	28.94	20.68	1588
14H-5, 100–103	172.70	26.88	18.95	1631
14H-6, 101–104	174.21	28.23	20.17	1594
15H-1, 102–105	176.22	27.98	20.31	1566
15H-2, 100–103	177.70	27.10	19.02	1638
15H-3, 115–118	179.35	28.21	19.11	1699
15H-4, 100–103	180.70	29.02	21.95	1483
15H-5, 100–103	182.20	28.42	19.56	1665
17X-1, 100–103	195.00	25.44	17.47	1698
17X-2, 100–103	196.50	25.31	19.52	1476
17X-3, 100–103	198.00	24.18	17.04	1659
17X-4, 30–33	198.80	27.67	19.12	1664
19X-1, 100–103	214.30	27.09	18.82	1658
19X-2, 100–103	215.80	27.53	18.94	1674
19X-3, 100–103	217.30	26.85	20.67	1467
19X-4, 100–103	218.80	28.59	19.32	1701
19X-5, 100–103	220.30	28.81	19.54	1692
19X-6, 100–103	221.80	28.37	19.16	1704
21X-1, 100–103	233.70	22.96	16.11	1683
21X-2, 100–103	235.20	27.28	20.92	1471
21X-3, 100–103	236.70	28.15	20.63	1546
22X-1, 100–103	243.30	29.18	21.51	1528
22X-2, 100–103	244.80	27.99	18.97	1700

Table 9. Vane-shear-strength data at Hole 824A.

Core, section, interval (cm)	Depth (mbsf)	Spring number	Torque (degrees)	Strain (degrees)	Shear strength (kPa)
133-824B-					
1H-1, 98–99	0.98	2	10	13	4.7
1H-3, 97–98	3.97	2	13	14	6.1
2H-1, 93–94	5.93	2	6	14	2.8
2H-2, 93–94	7.43	2	4	6	1.9
2H-3, 88–89	8.88	2	14	14	6.6
2H-4, 108–109	10.58	2	13	12	6.1
2H-5, 93–94	11.93	2	5	5	2.4
3H-1, 91–92	15.41	2	17	10	8.0
3H-2, 91–92	16.91	2	11	8	5.2
3H-3, 91–92	18.41	2	11	15	5.2
3H-4, 91–92	19.91	2	11	6	5.2
3H-5, 91–92	21.41	2	7	3	3.3
3H-6, 91–92	22.91	2	8	2	3.8
4H-1, 95–96	24.95	2	8	7	3.8
4H-2, 95–96	26.45	2	12	13	5.6
4H-3, 95–96	27.95	2	5	7	2.4
4H-4, 95–96	29.45	2	4	3	1.9
4H-5, 95–96	30.95	2	4	2	1.9
4H-6, 95–96	32.45	2	4	4	1.9
5H-1, 95–96	34.45	2	7	3	3.3
5H-2, 95–96	35.95	2	4	2	1.9
5H-3, 95–96	37.45	2	6	5	2.8
5H-4, 95–96	38.95	2	6	5	2.8
5H-5, 95–96	40.45	2	8	10	3.8
5H-6, 98–99	41.98	2	6	4	2.8
6H-3, 92–93	46.92	2	5	6	2.4
6H-4, 81–82	48.31	2	7	7	3.3
6H-5, 81–82	49.81	2	18	15	8.5
6H-6, 81–82	51.31	2	11	10	5.2
133-824A-					
1H-1, 90–91	50.90	2	5	10	2.4
1H-2, 90–91	52.40	2	4	3	1.9
1H-3, 90–91	53.90	2	2	1	0.9
1H-4, 90–91	55.40	2	3	2	1.4
1H-5, 90–91	56.90	2	4	4	1.9
1H-6, 90–91	58.40	2	4	2	1.9
2H-1, 90–100	60.40	2	3	4	1.4
2H-2, 99–100	61.99	2	5	3	2.4
2H-3, 99–100	63.49	2	10	9	4.7
2H-4, 99–100	64.99	2	9	9	4.2
2H-6, 90–91	67.90	2	7	7	3.3
3H-2, 95–96	71.45	2	4	4	1.9
3H-4, 95–96	74.45	2	1	2	0.5
3H-5, 95–96	75.95	2	6	3	2.8
3H-6, 95–96	77.45	2	12	3	5.6
5H-1, 95–96	88.95	2	11	5	5.2
5H-2, 95–96	90.45	2	9	18	4.2
5H-3, 95–96	91.95	2	4	3	1.9
5H-4, 95–96	93.45	2	6	1	2.8
5H-5, 95–96	94.95	2	7	6	3.3
5H-6, 95–96	96.45	2	20	13	9.4
6H-1, 96–97	98.46	2	5	4	2.4
6H-2, 96–97	99.96	2	18	14	8.5
6H-3, 107–108	101.57	2	7	8	3.3
6H-4, 107–108	103.07	2	27	19	12.7
6H-5, 107–108	104.57	2	8	6	3.8
7H-1, 107–108	108.07	2	10	8	4.7
7H-2, 107–108	109.57	2	5	10	2.4
7H-3, 107–108	111.07	2	5	3	2.4
7H-6, 107–108	115.57	2	15	15	7.1
7H-7, 57–58	116.57	2	14	16	6.6
8H-1, 107–108	117.57	2	8	10	3.8
8H-2, 107–108	119.07	2	14	8	6.6
8H-3, 107–108	120.57	2	2	7	0.9
8H-5, 107–108	123.57	2	9	6	4.2
8H-6, 103–104	125.03	2	4	3	1.9
9H-1, 101–102	127.01	2	14	11	6.6
9H-2, 101–102	128.51	2	20	5	9.4
9H-3, 88–89	129.88	2	6	8	2.8
14H-2, 88–89	168.08	2	17	14	8.0
14H-3, 94–95	169.64	2	24	13	11.3
14H-4, 94–95	171.14	2	15	13	7.1
14H-5, 88–89	172.58	2	19	14	8.9
14H-6, 92–93	174.12	2	20	13	9.4
15H-1, 93–94	176.13	2	33	25	15.5
15H-2, 93–94	177.63	2	16	13	7.5
15H-3, 97–98	179.17	2	6	9	2.8
15H-4, 92–93	180.62	2	6	13	2.8

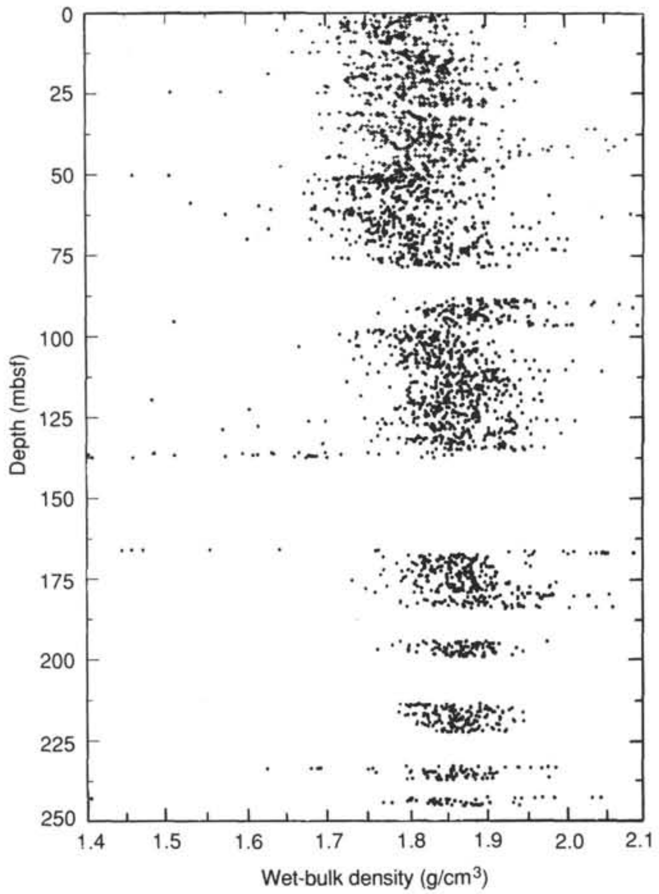

Figure 16. GRAPE bulk-density measurements for Site 824. Data values have been averaged at 5-cm intervals. (●) indicates data from Hole 824A, and (+) indicates data from Hole 824B.

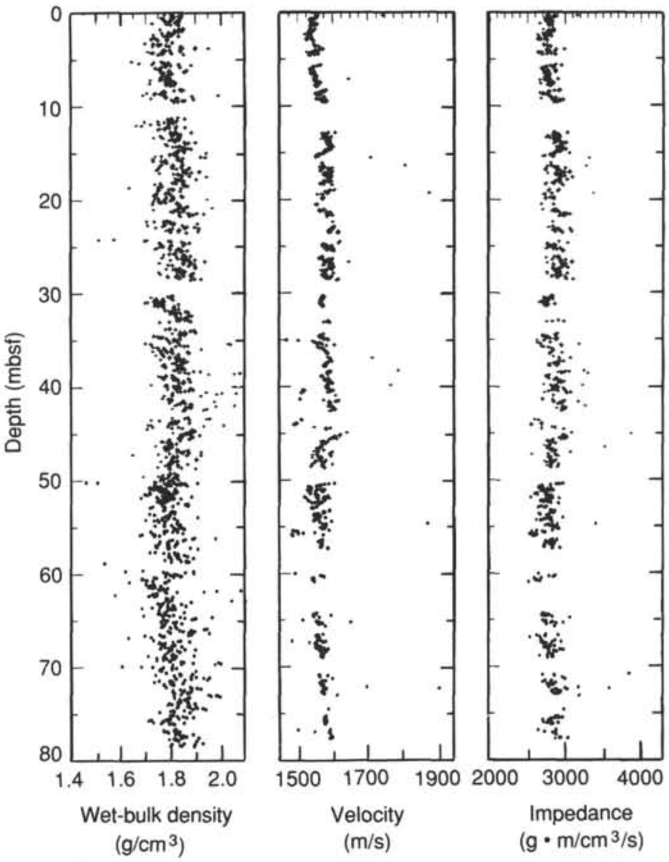

Figure 17. GRAPE wet-bulk density, MST sonic velocity, and impedance calculated as a product of sonic velocity and bulk density. (●) indicates data from Hole 824A, and (+) indicates data from Hole 824B.

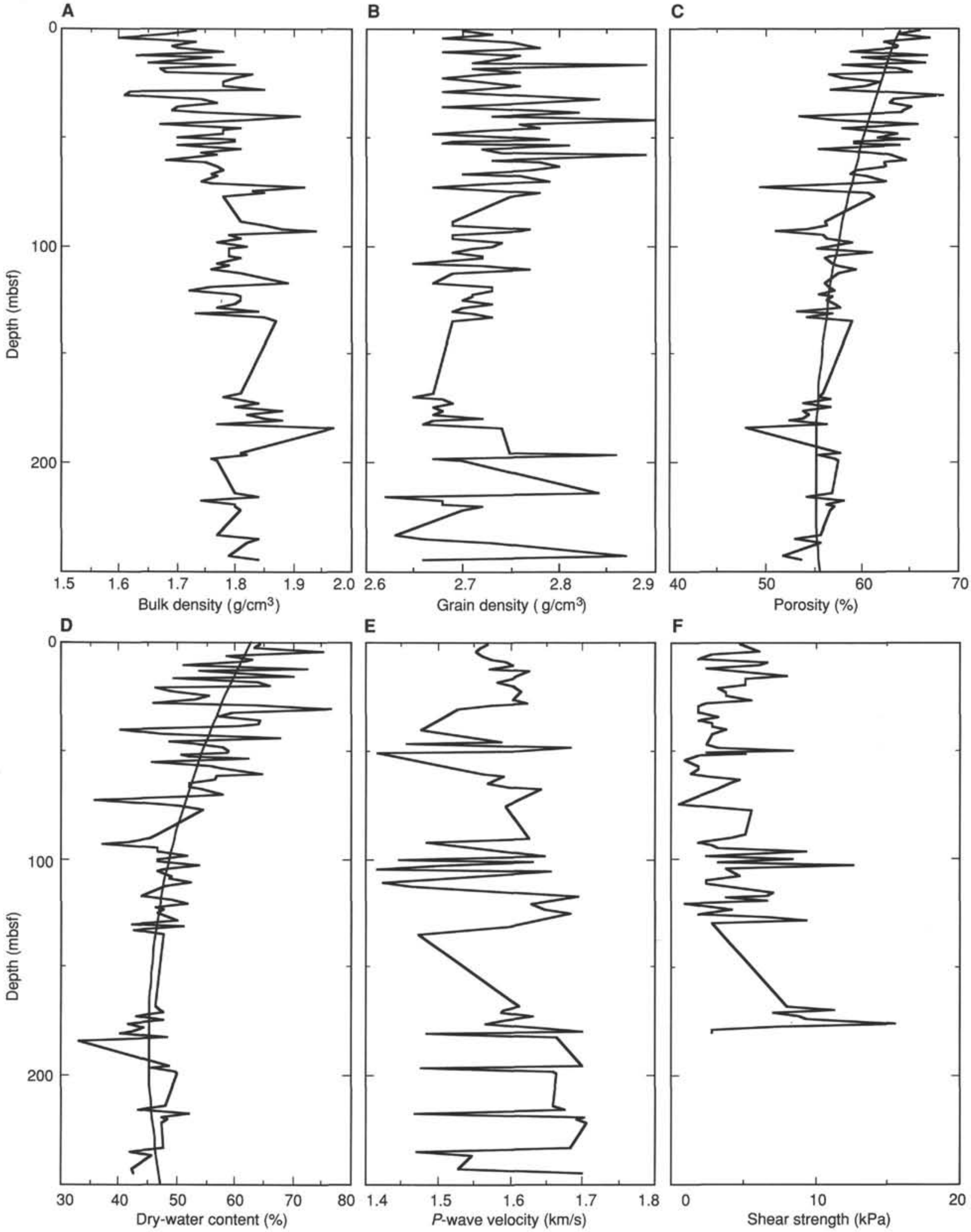

Figure 18. Physical properties vs. depth, Site 824. **A.** Bulk density; data were obtained from mass and volume measurements on samples taken from split cores. **B.** Grain density. **C.** Porosity; data were obtained from mass and volume measurements of samples taken from split cores. The 2nd order regression curve is of the form porosity $P = 64 - 0.091 \times Z + 0.00022 \times Z^2$, where Z is depth and the regression coefficient $R = 0.709$. **D.** Dry-water content; data were obtained from mass and volume measurements on samples taken from split cores. The 2nd order regression curve is of the form $DW = 63 - 0.21 \times Z + 0.000566 \times Z^2$, where DW = dry-water content, Z = depth, and the regression coefficient $R = 0.689$. **E.** *P*-wave velocity; data were obtained from samples taken from split cores using the Hamilton Frame. **F.** Shear strength; data were obtained from split cores using the Wykeham-Farrance motorized vane apparatus on the split cores.

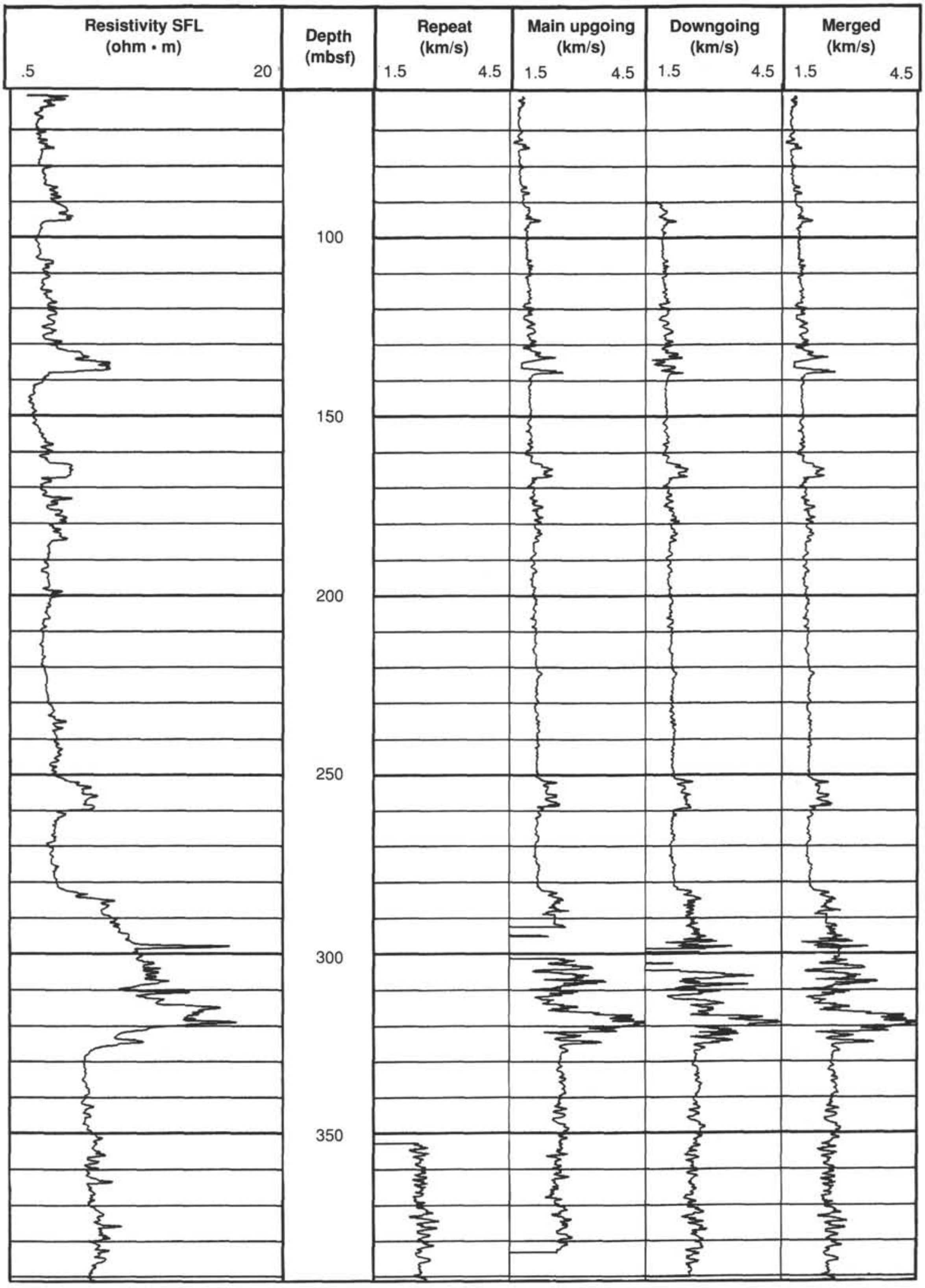

Figure 19. Velocity and resistivity logs for Site 824. The most reliable portions of three sonic log runs (downgoing, upgoing repeat section, and main upgoing logs), each with some unreliable data, are merged into the composite log at far right. Note that the merged log still has some intervals that are untrustworthy, based on comparison to resistivity.

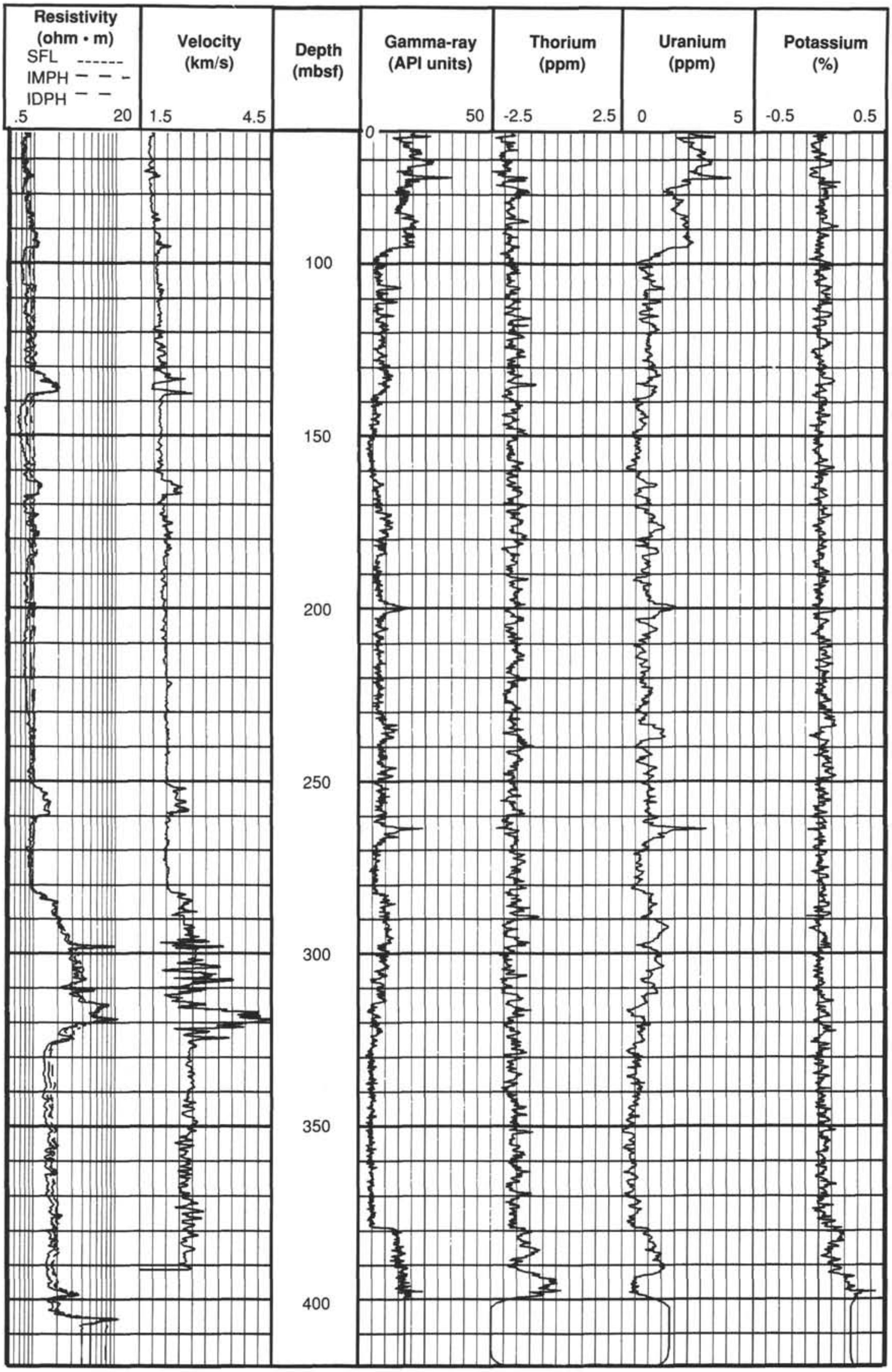

Figure 20. Primary downhole logs from Site 824.

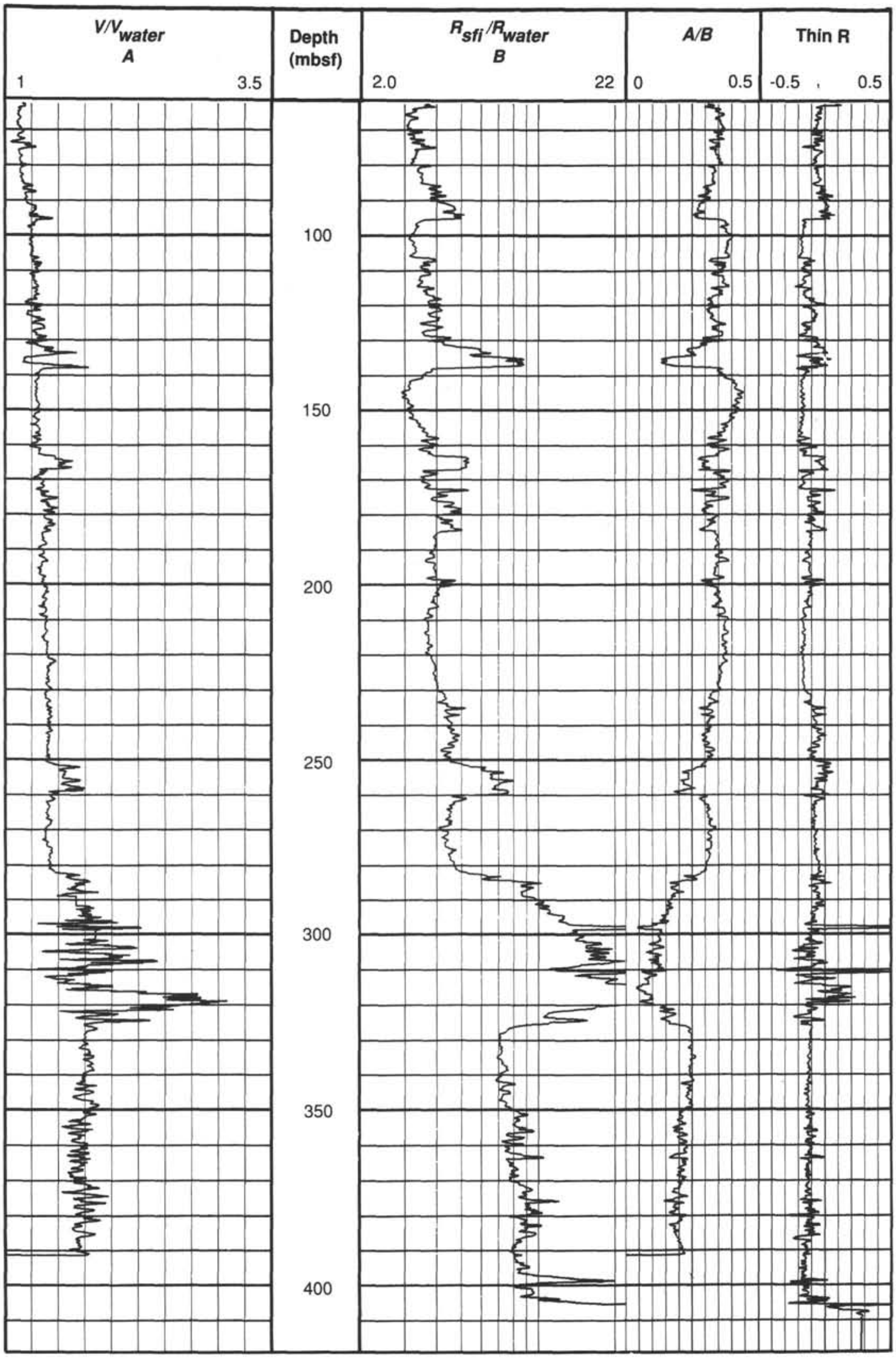

Figure 21. Velocity and resistivity for Site 824, plotted as ratios in order to highlight variations in cementation.

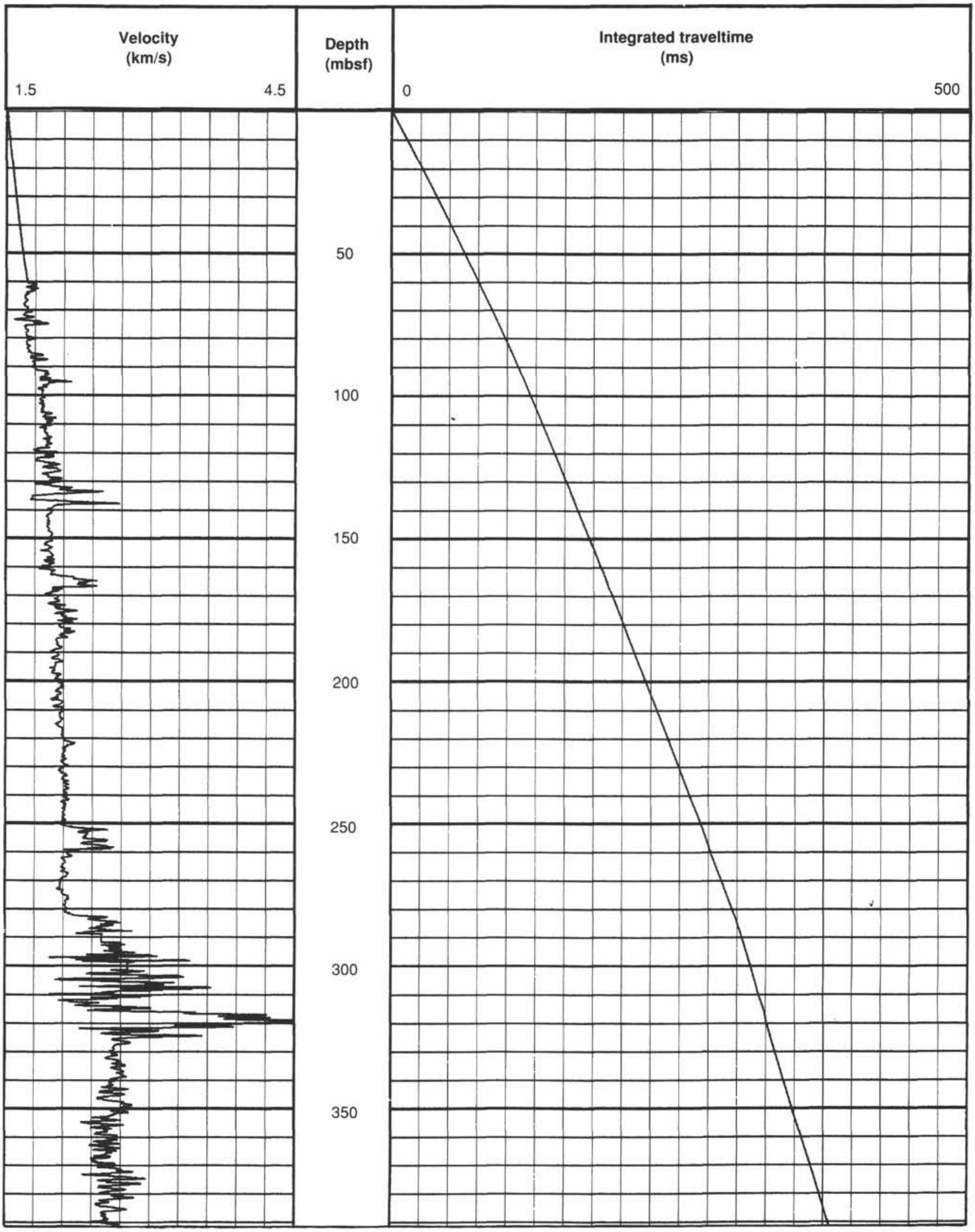

Figure 22. Velocity log and the integrated two-way traveltime function that it implies, for comparison of core-based information from Site 824 with the seismic sections across the site.

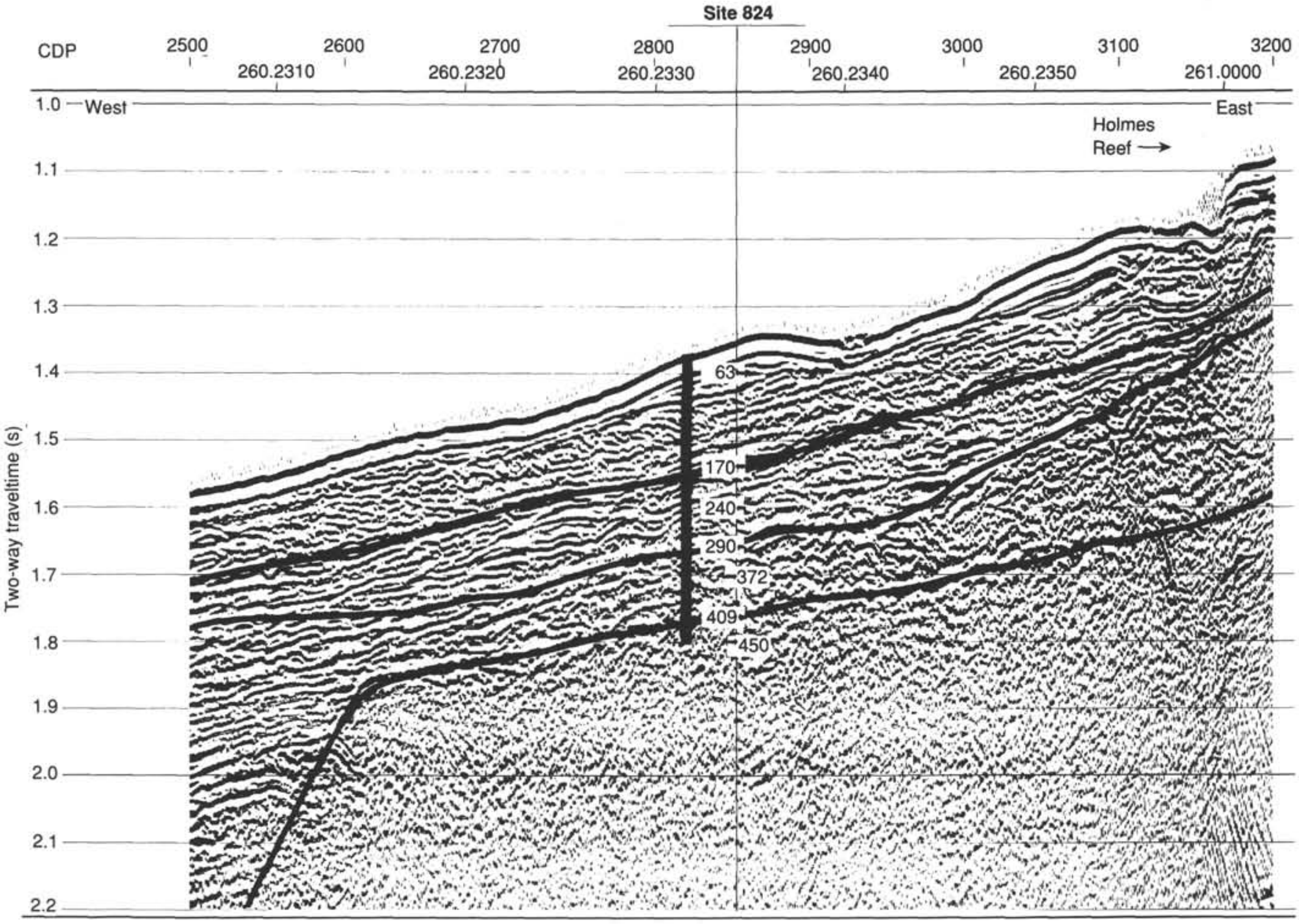

Figure 23. Seismic section from east to west through Site 824.

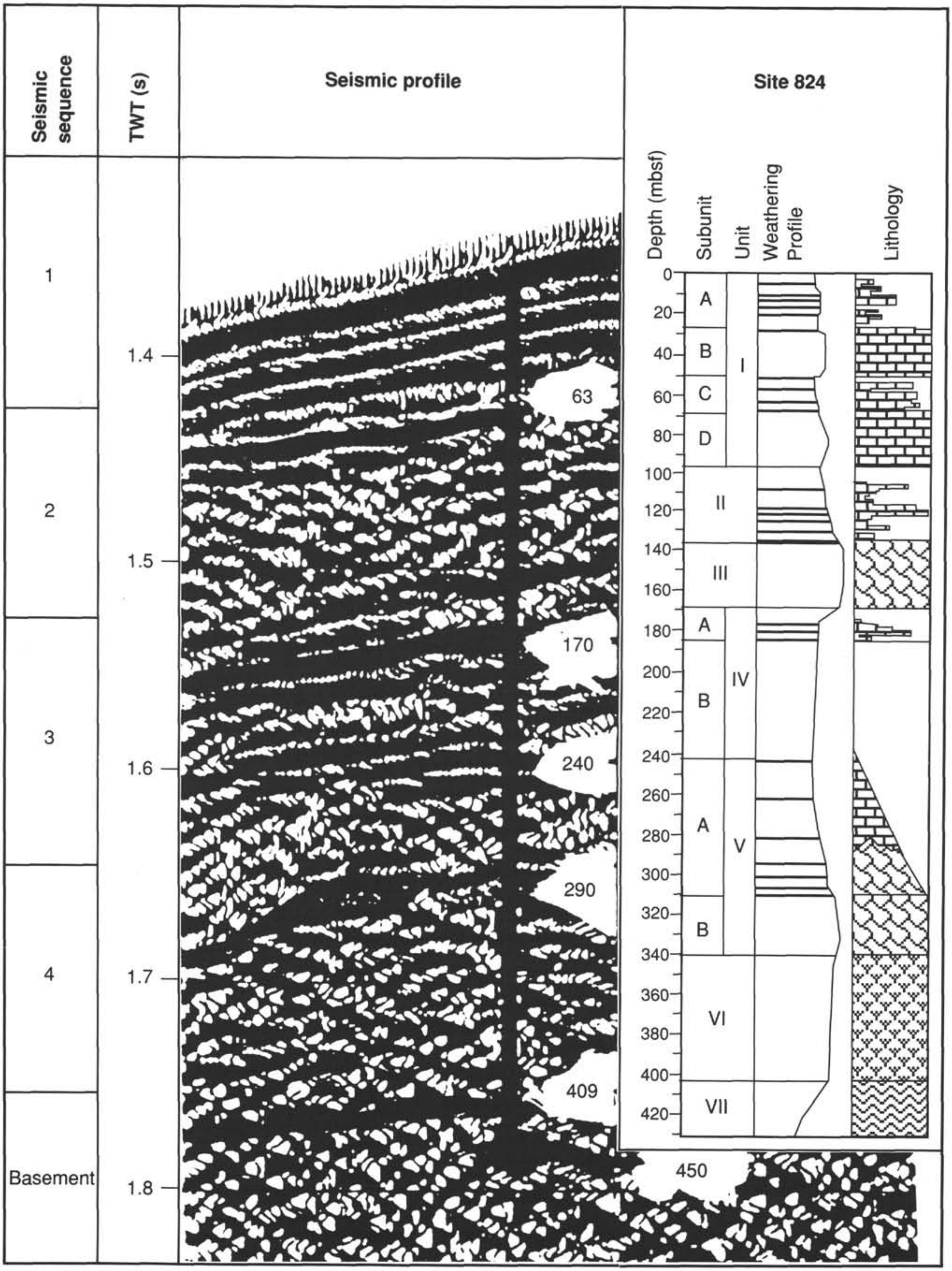

Figure 24. Seismic and lithostratigraphic sequences at Site 824.

Hole 824D: Resistivity-Sonic-Natural Gamma Ray Log Summary

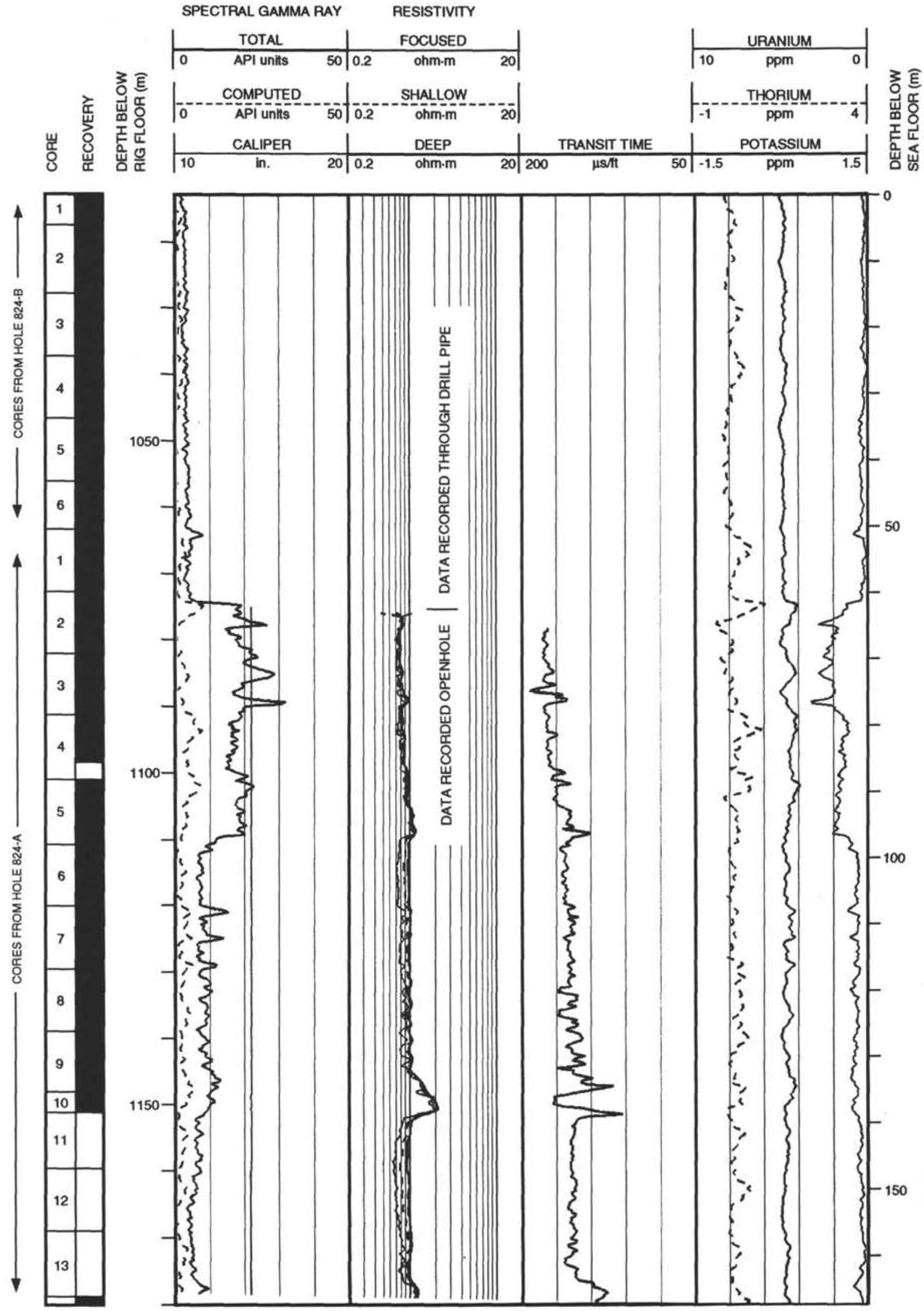

Hole 824D: Resistivity-Sonic-Natural Gamma Ray Log Summary (continued)

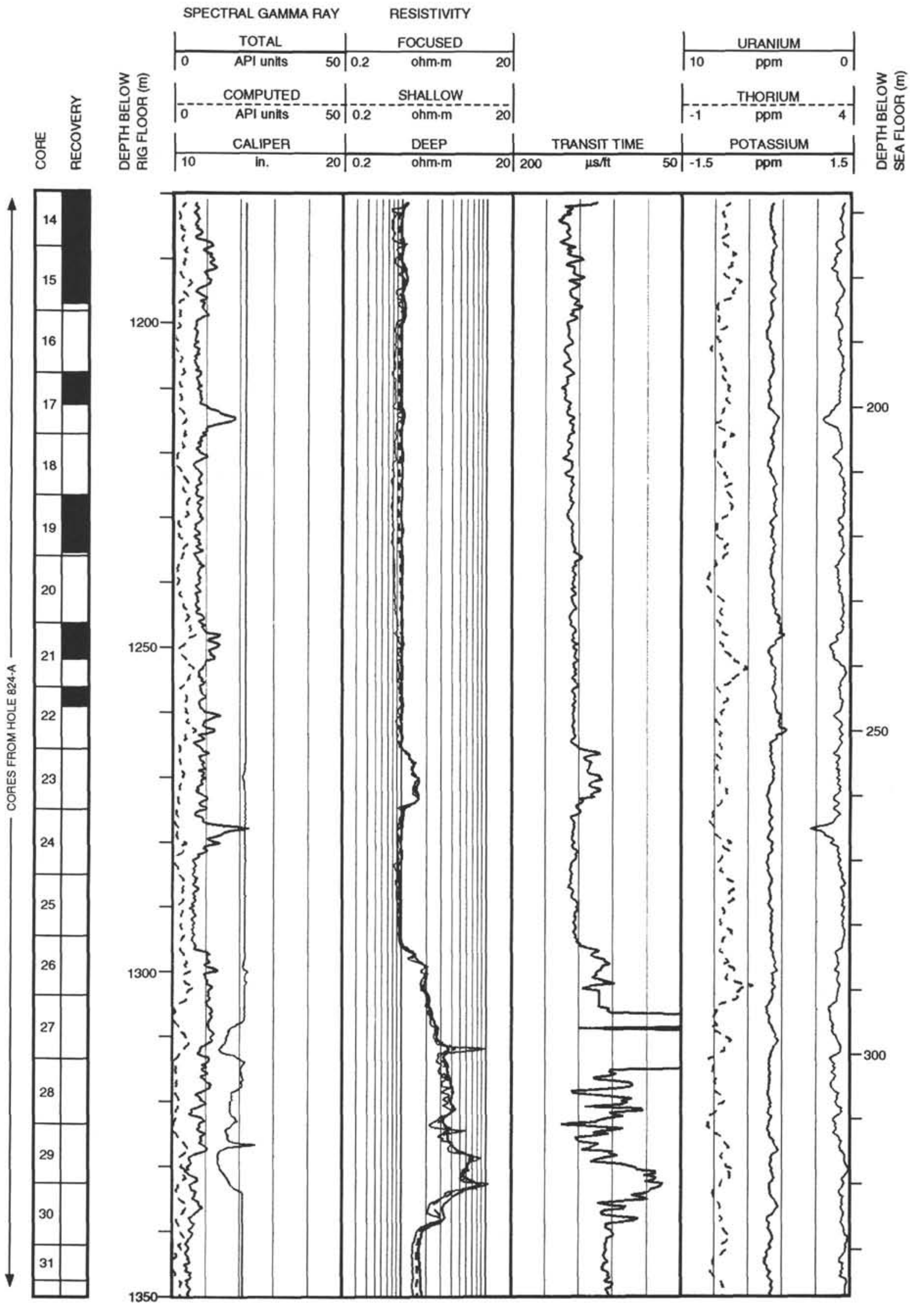

Hole 824D: Resistivity-Sonic-Natural Gamma Ray Log Summary (continued)